Mesure de la Déformation par Imagerie Satellitaire

« InSAR monitoring of surface displacements and detection of abnormal behaviour for a geothermal operation, case of the Landau power plant (Germany) »

Eric HENRION, Cécile DOUBRE, Frédéric MASSON

IPGS / EOST

1. INTRODUCTION

- Underground reservoirs
  - Oil production
  - Deep geothermal
  - Natural gas storage
  - …

- Surface deformation
  - Uplift around injection well
  - Subsidence around production well

- Surface deformation monitoring
  - Condition (pressure / volume)
  - Environment (flow migration, permeability, rheology)
  - **Detection of abnormal behaviour (prevention)**

- Monitoring tools
  - GNSS (high-temporal resolution)
  - **SAR interferometry (high-spatial resolution)**

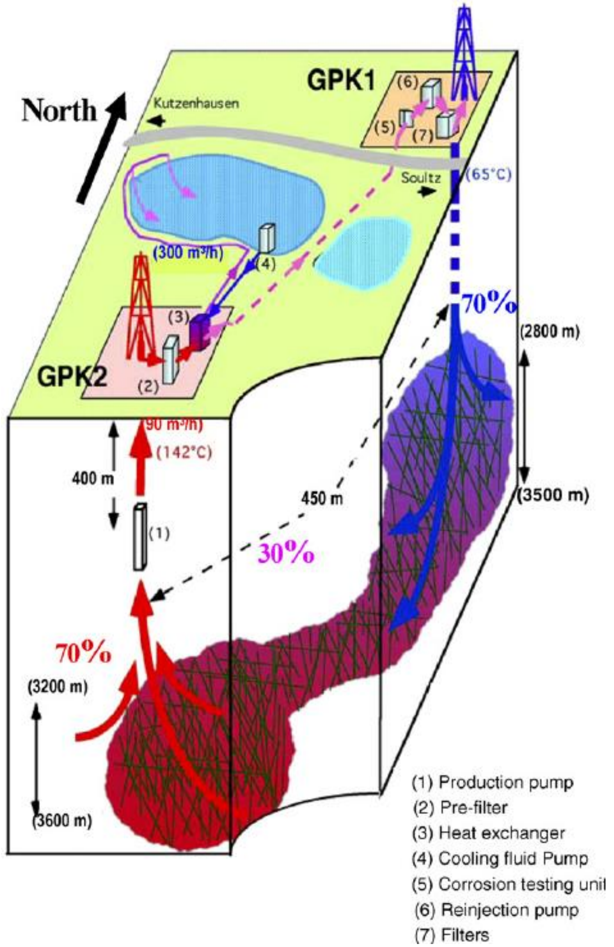

Fig 1. Example of an EGS with an injection wells (GPK1) and a production wells (GPK2) (*Gerard et al., 2006*).

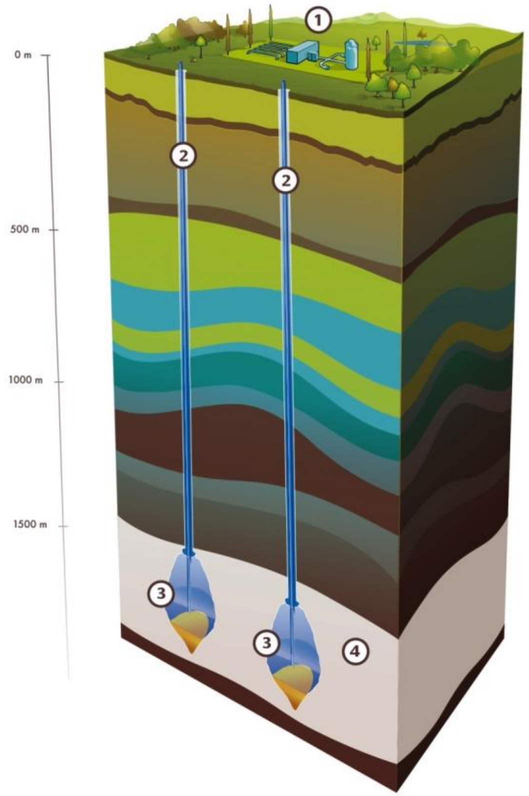

Fig 2. Natural gas storage in salt caverns (www.storengy.com).

3. CONTEXT

- Landau in Germany (80 km north of Strasbourg, France)
  - Underground of the city exploited for:
    - Deep geothermal in south (electricity and heat)
    - Oil production in east and north

- EGS power plant
  - Project initiated in 2000, and started in 2007
  - 2 wells at about 3000 m depth

- Known case of accident
  - Occurred in **June 2013**
  - Leak in injection wells at ~450 m depth (*Heimlich et al., 2015*)
  - Power plant shutdown in **March 2014**
  - Restart of the power plant in **October 2017**

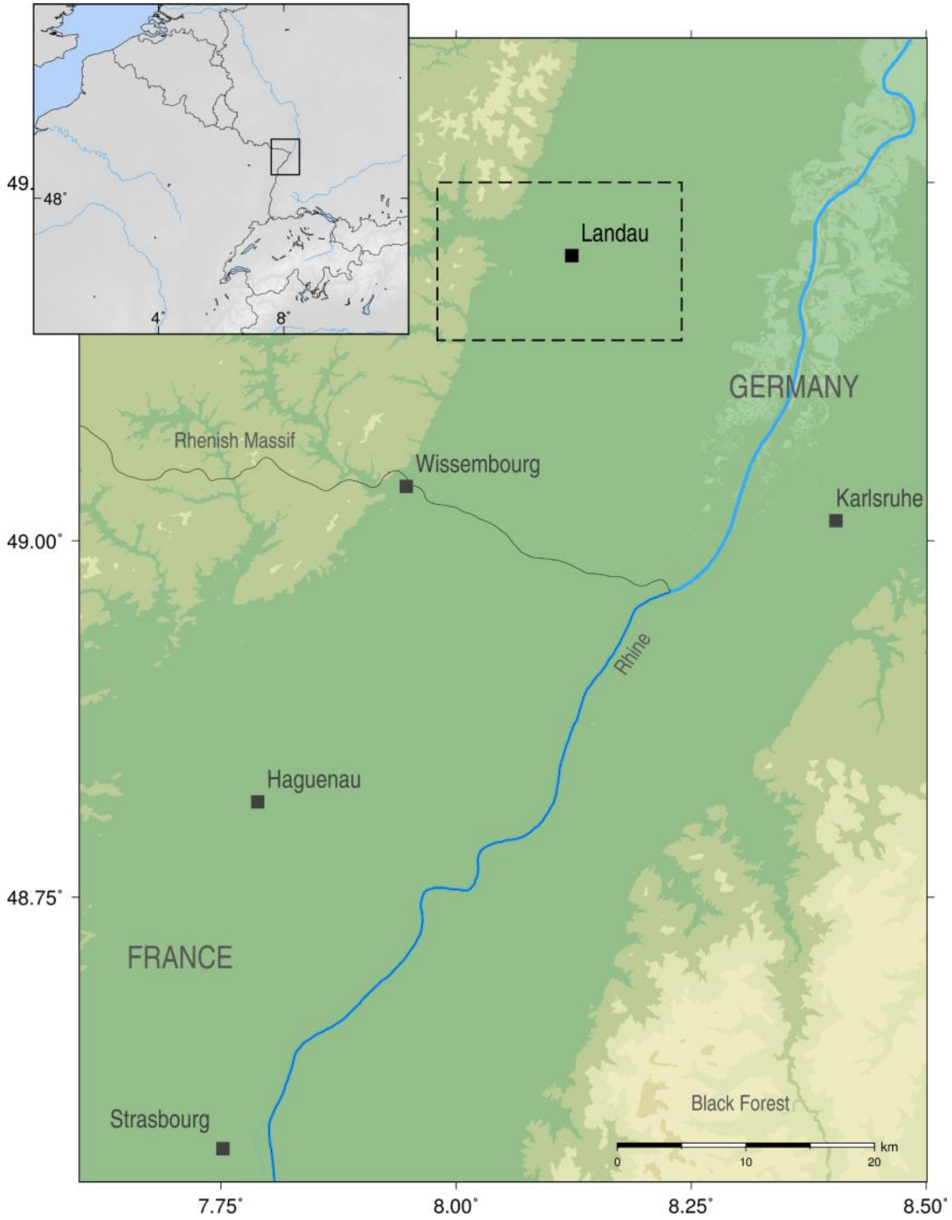

Fig 3. Localisation of Landau, the black rectangle represents the studied area.

- Dataset
  - TerraSAR-X
  - 125 X-band images (λ = 3.1 cm)
  - Repeat period : 11 days

- Processing
  - PS-InSAR : StaMPS (*Hooper et al., 2012*)
  - Persistent scatterers (urban areas)
  - Lock : temporal decorrelation (vegetated areas)

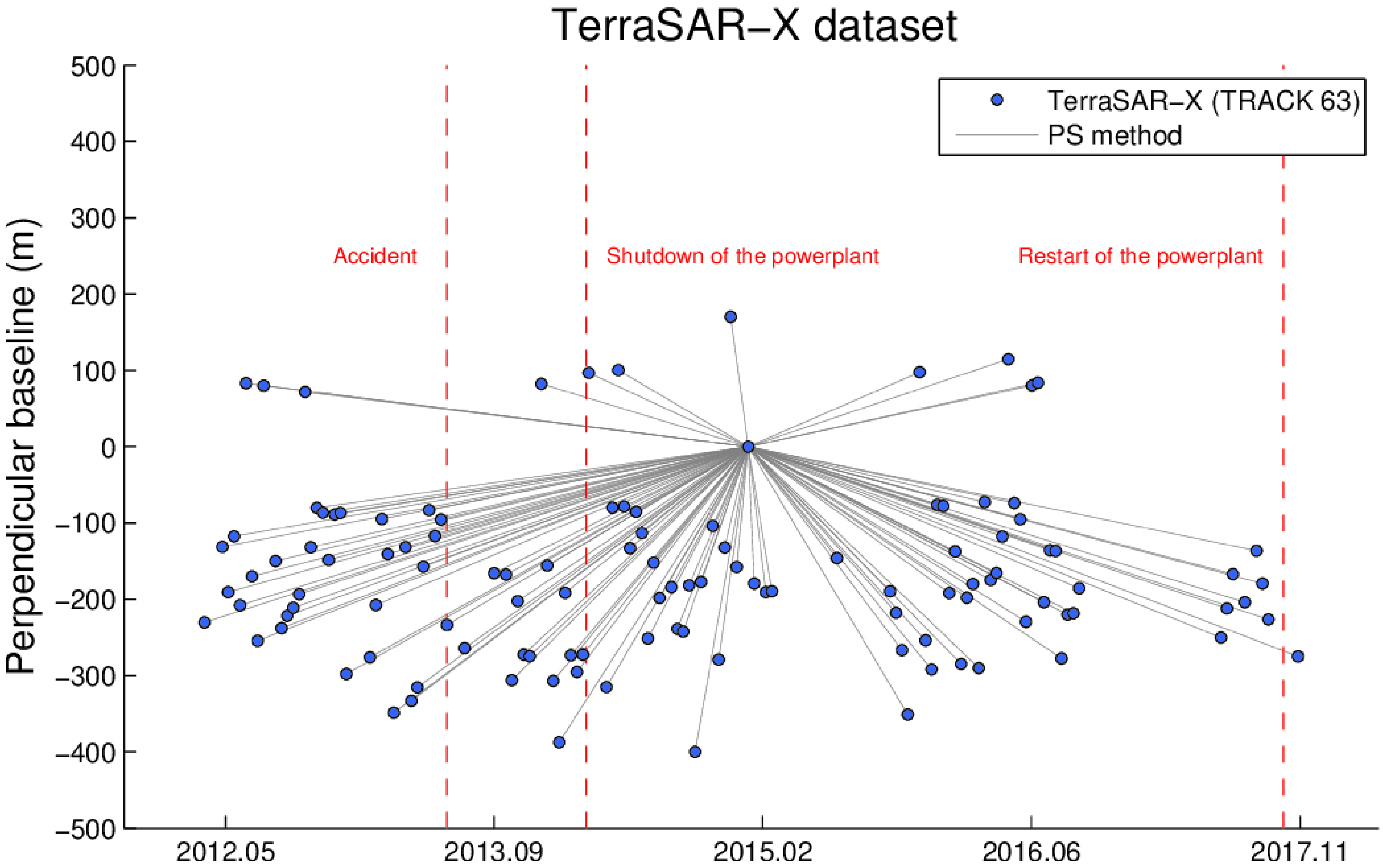

Fig 4. TerraSAR-X dataset: perpendicular baselines as a function of time. Red lines: accident, shutdown and restart of the power plant.

4. RESULTS

- Spatial analysis

- Period 1
  - Cumulated LOS displacements
  - Pixels in urban areas (PS)

- Uplift in north (~13 mm LOS)
- Subsidence in east (~8 mm LOS)
- Stable geothermal site (~2 mm LOS)

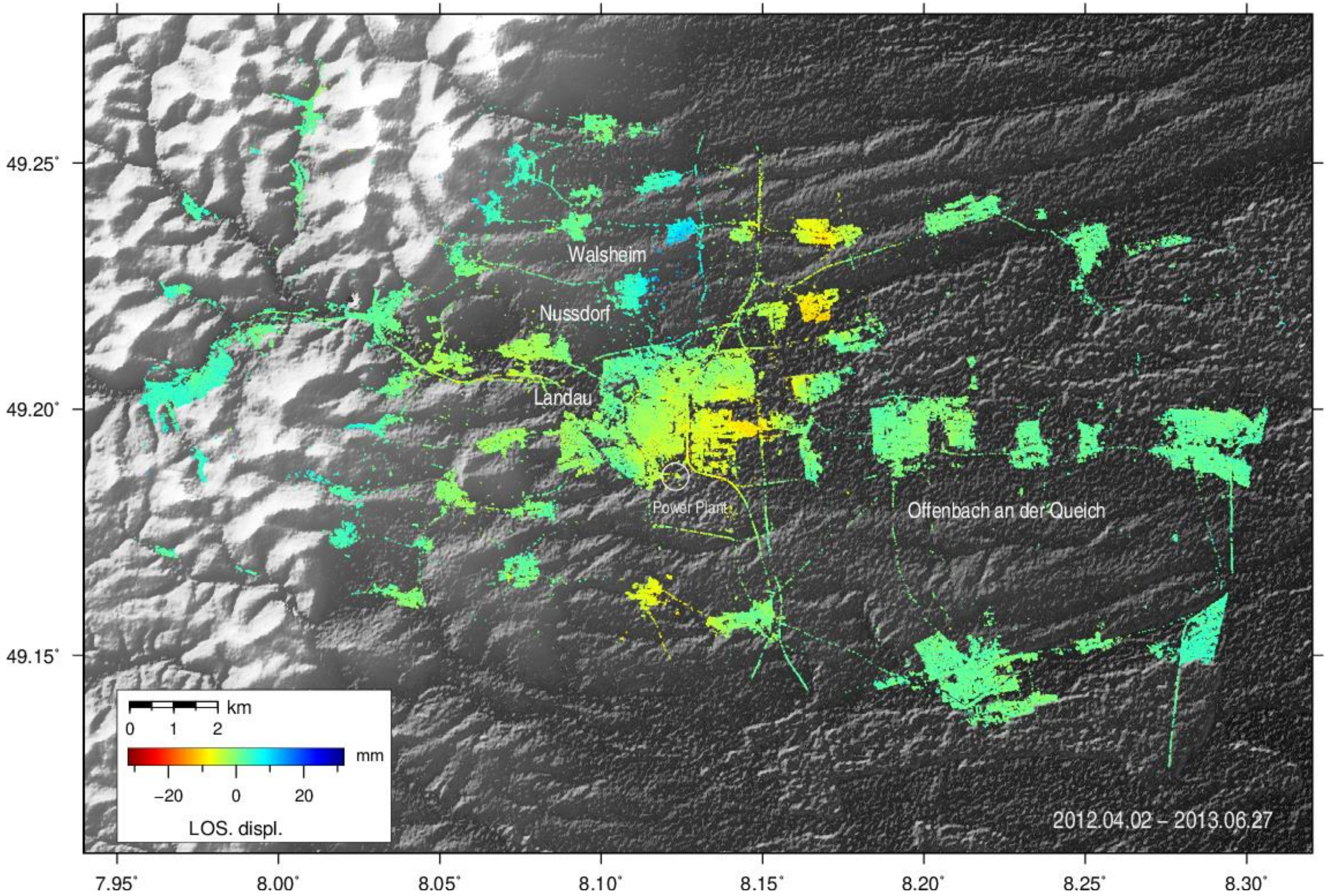

Fig 5. Cumulated LOS displacements, period 1: 2012.04.02 – 2013.06.27.

4. RESULTS

- Spatial analysis

- Period 2
  - Cumulated LOS displacements
  - Pixels in urban areas (PS)

- Uplift
  - Geothermal power plant (~33 mm LOS)
  - Spread over the city (~10 mm LOS)

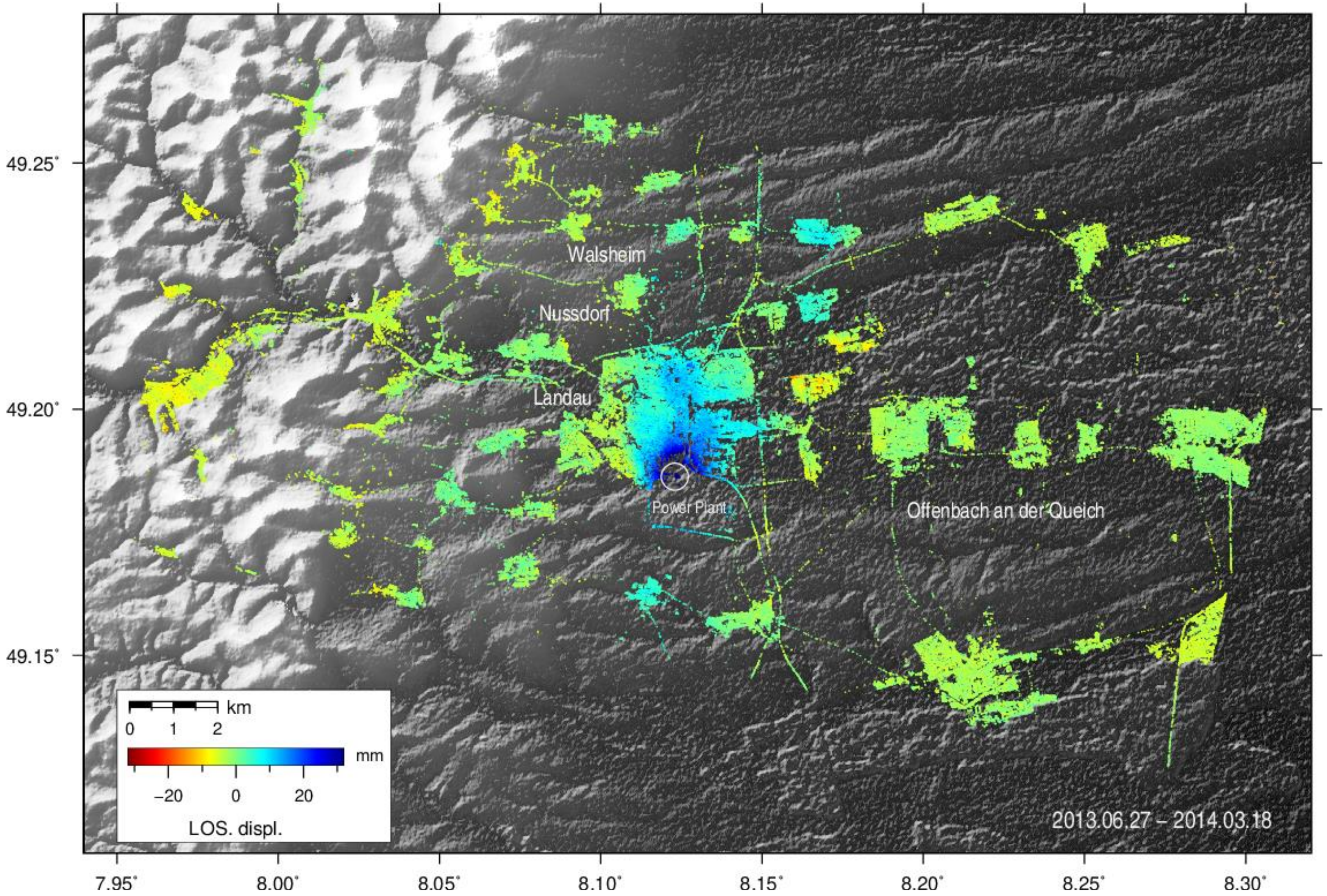

Fig 6. Cumulated LOS displacements, period 2: 2013.06.27 – 2014.03.18.

4. RESULTS

- Spatial analysis

- Period 3
  - Cumulated LOS displacements
  - Pixels in urban areas (PS)

- Subsidence
  - Geothermal power plant (~25 mm LOS)
  - Spread over the city (~8 mm LOS)
  - North (~17 mm LOS)

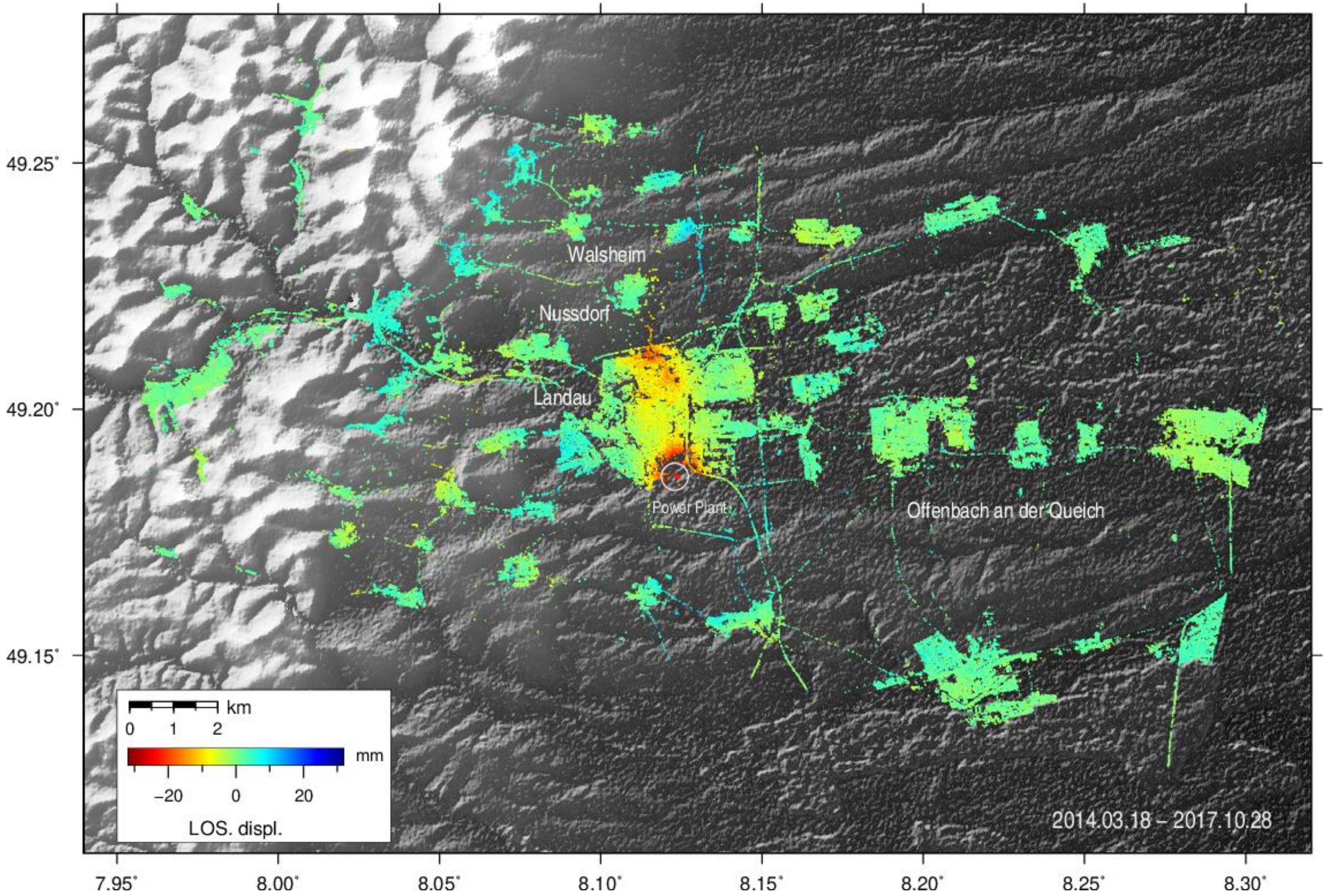

Fig 7. Cumulated LOS displacements, period 3: 2014.03.18 – 2017.11.19

4. RESULTS

- Analyse spatiale

- Full period
  - Cumulated LOS displacements
  - Pixels in urban areas (PS)

- Boreholes
  - North (oil production)
  - East (oil production)

- http://www.geopotenziale.org

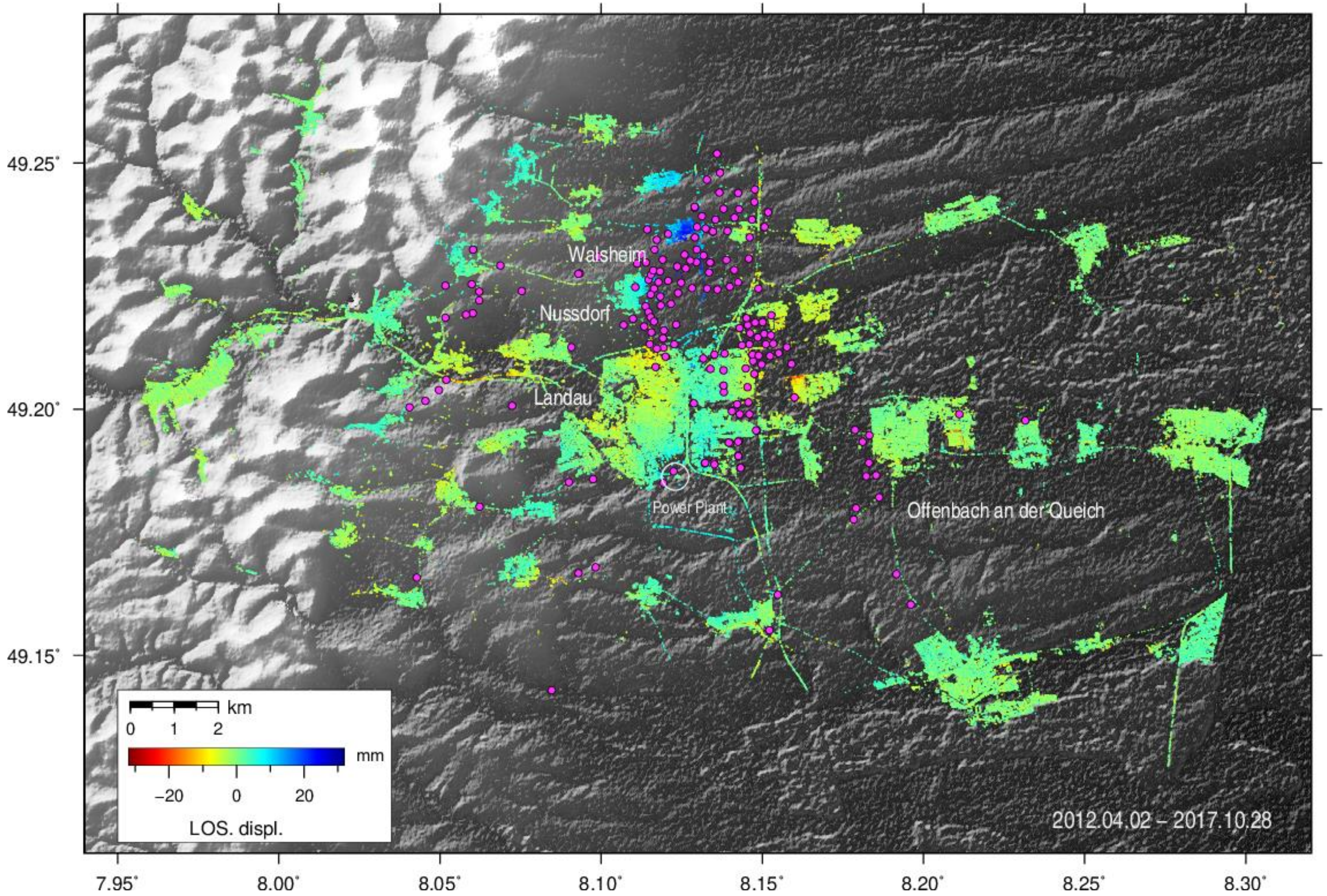

Fig 8. Cumulated LOS displacements, full period: 2012.04.02 – 2017,10,28. Purple: geothermal and oil boreholes.

- Temporal analysis

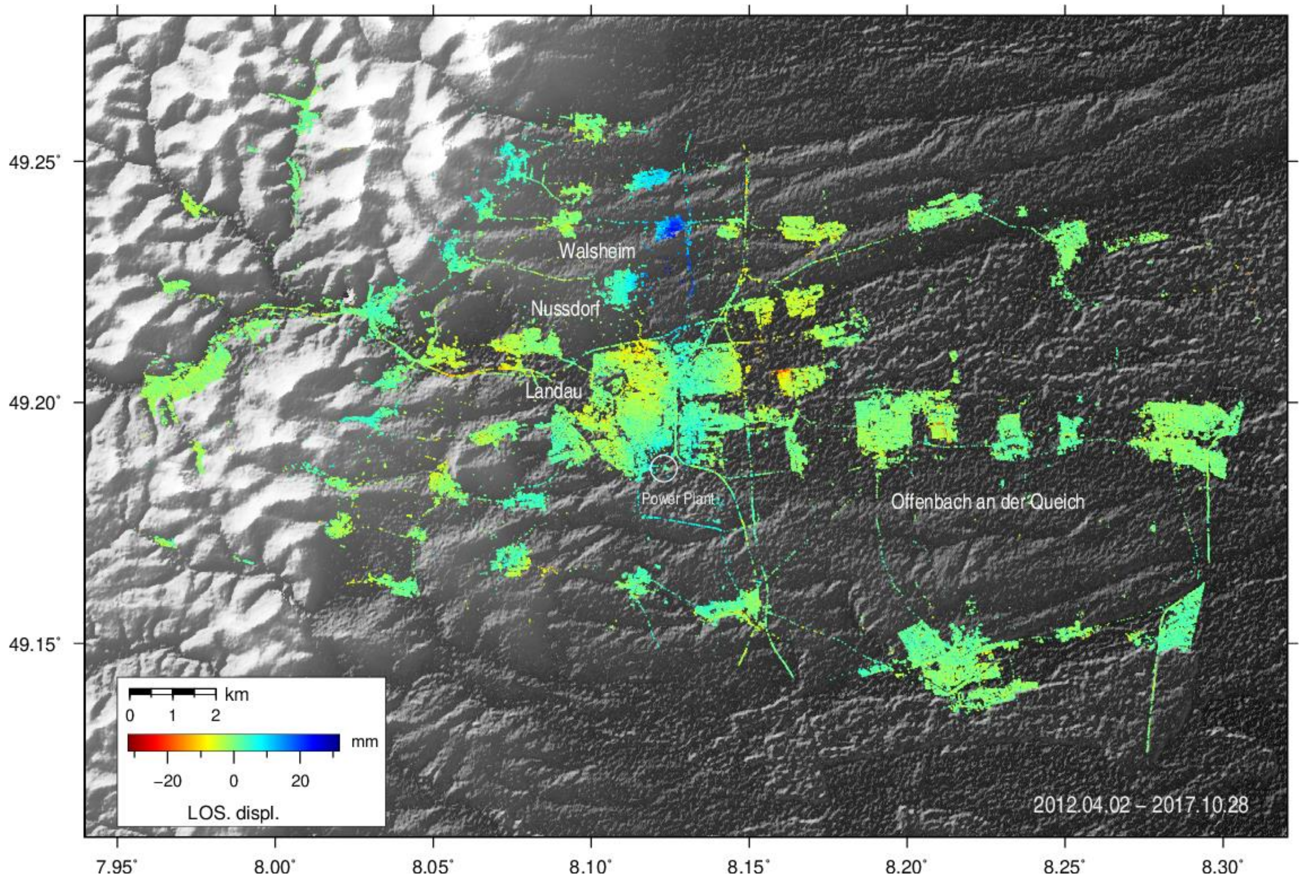

Fig 9. Cumulated LOS displacements, 2012.04.02 – 2017.10.28.

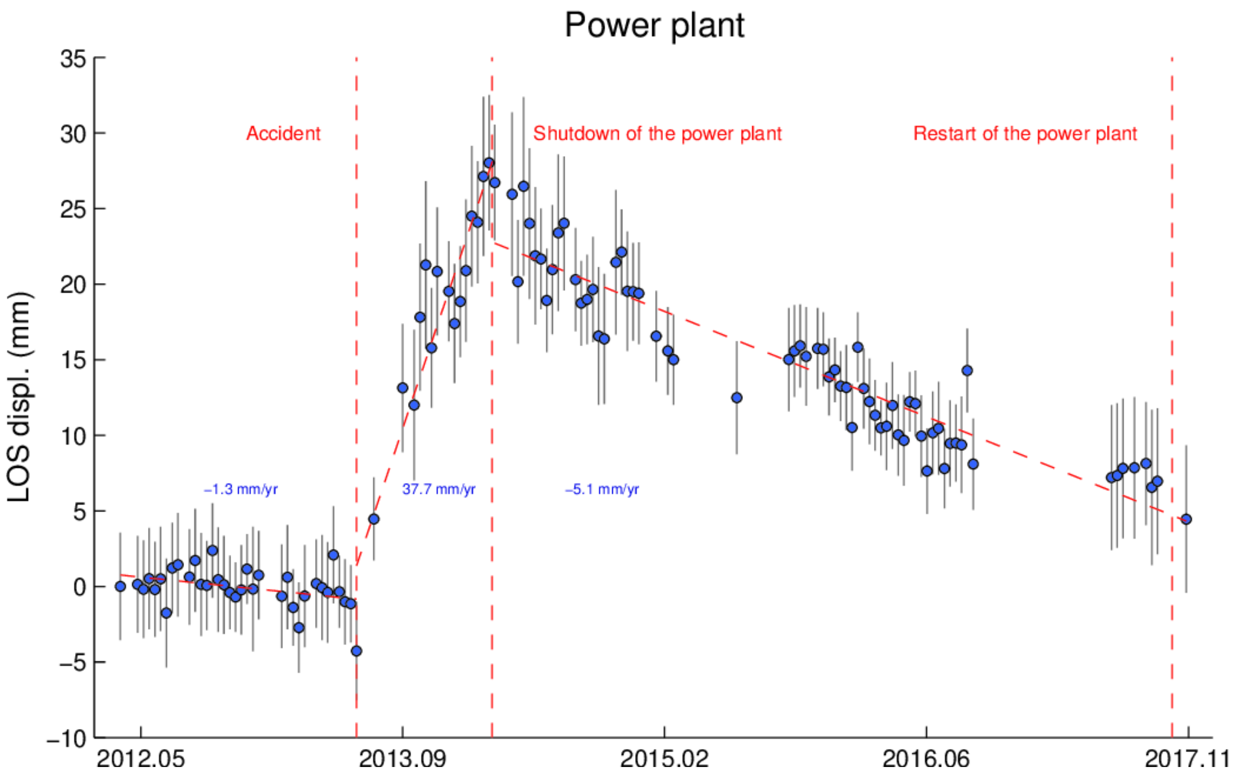

Fig 10. Time series of cumulated LOS displacements at the power plant location.

- **Motivation**
  - Important archive: TerraSAR-X with high-temporal sampling (11 days ≈ Sentinel-1) with a time span of about 5.5 years
  - Monitoring of the event: period of calm, occurrence of the accident, and post-accident
  - Known affected spatial area (*Heimlich et al., 2015*)
  - Processing chain : StaMPS (*Hooper et al., 2012*)
- StaMPS :

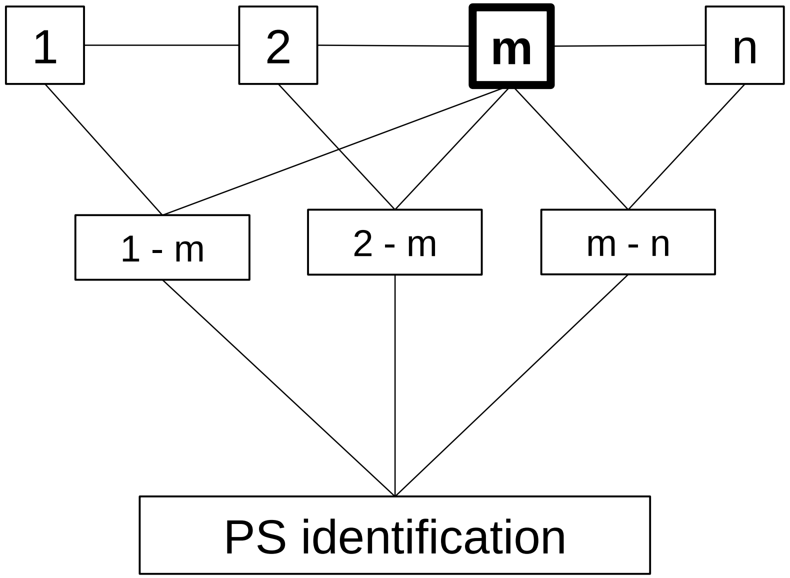

- **Motivations**
  - Important archive: TerraSAR-X with high-temporal sampling (11 days ≈ Sentinel-1) with a time span of about 5.5 years
  - Monitoring of the event: period of calm, occurrence of the accident, and post-accident
  - Known affected spatial area (*Heimlich et al., 2015*)
  - Processing chain : StaMPS (*Hooper et al., 2012*)
- StaMPS: **new PS identification over time**

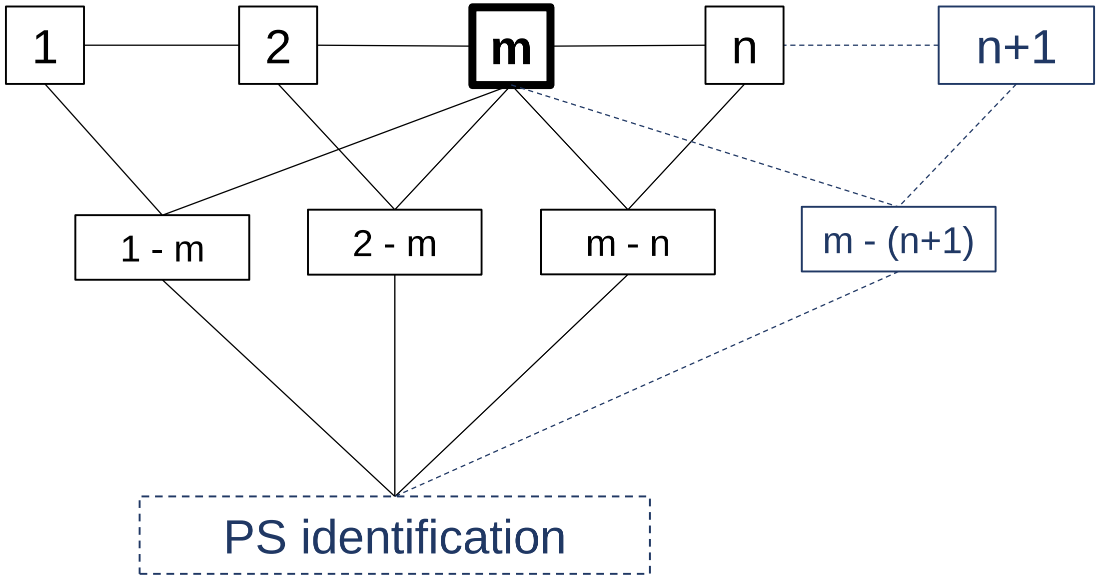

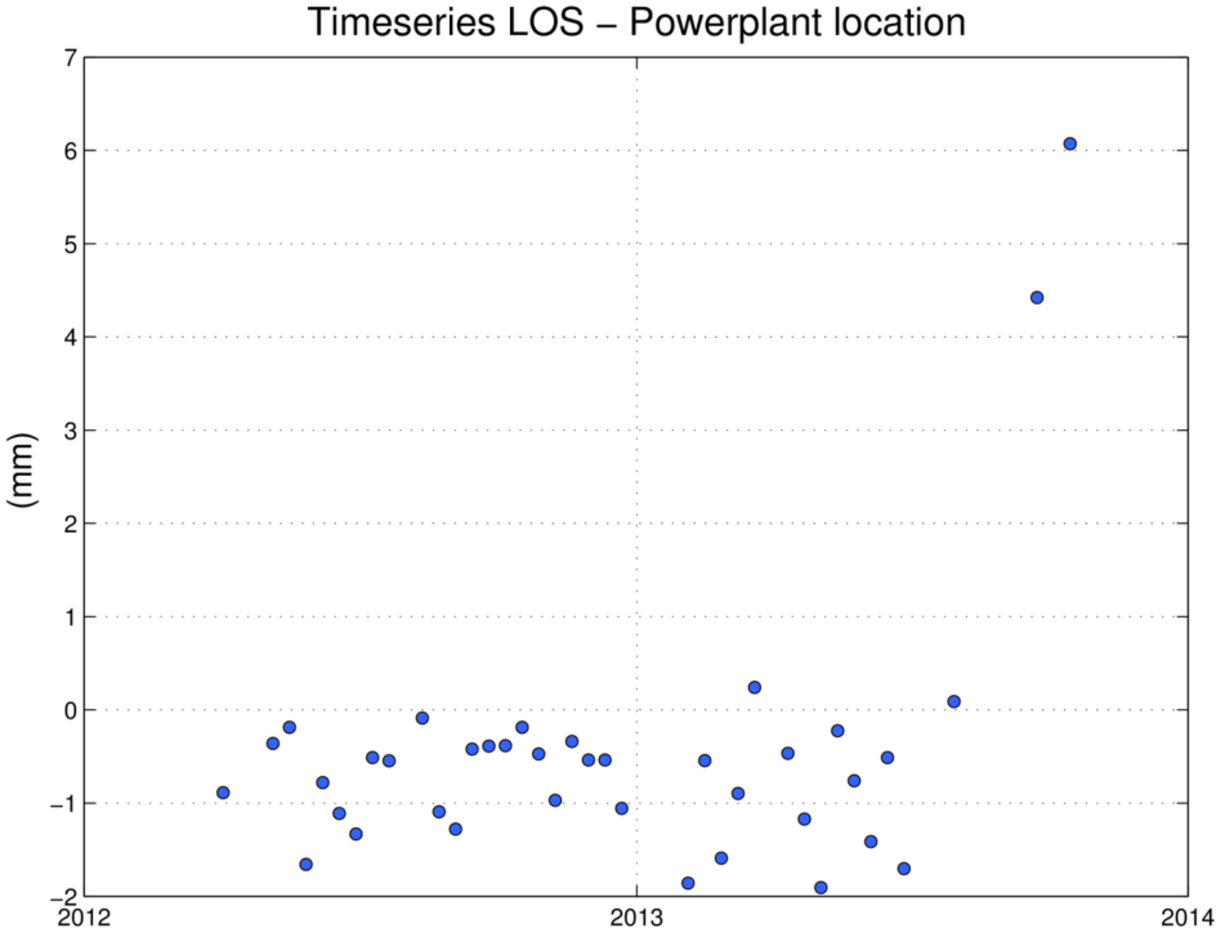

Fig 11. Time series of cumulated LOS displacements at power plant location.

- Monitoring tool : Independent Component Analysis (ICA)

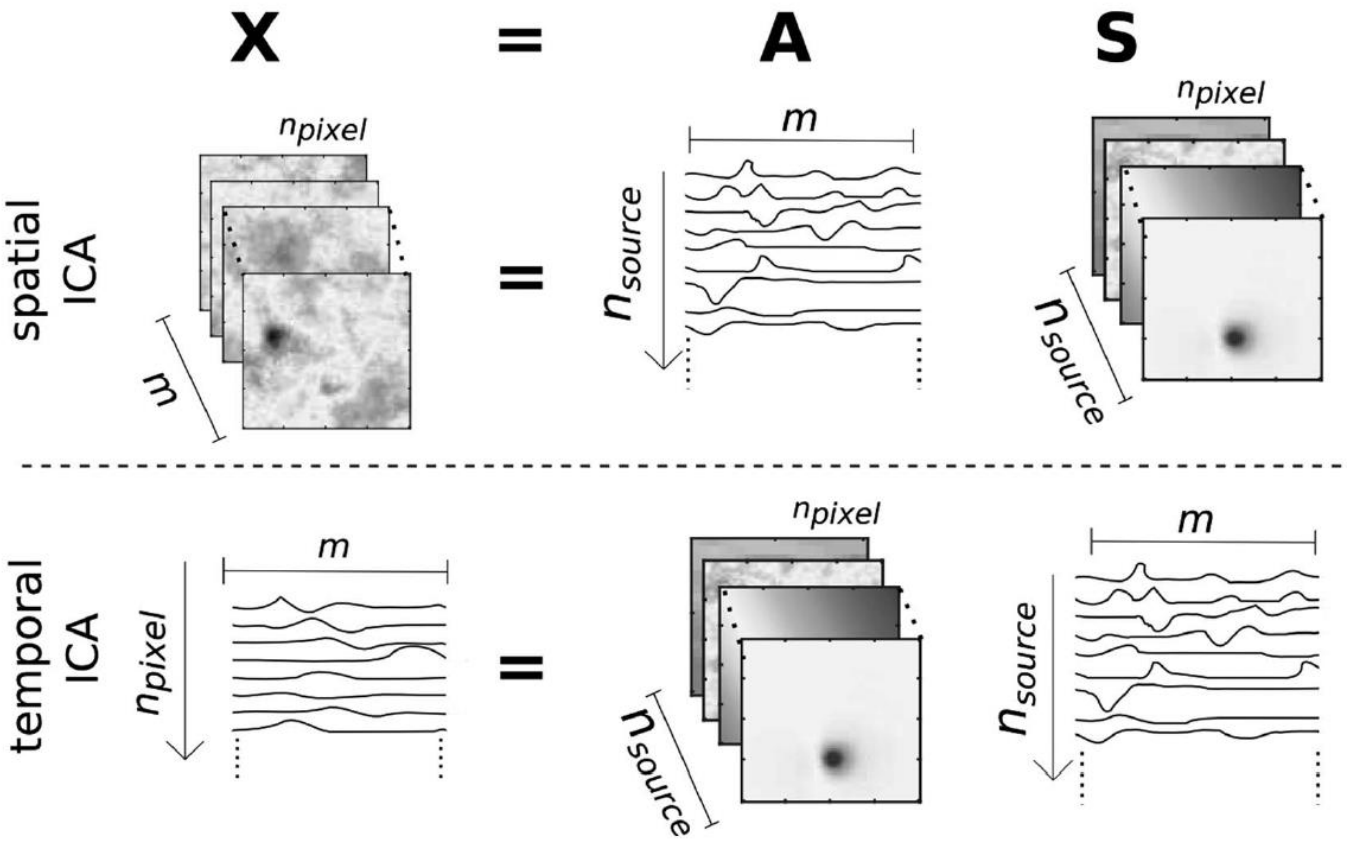

Fig 12. ICA linear problem. X: observations (interferograms), A: mixing vectors, S: sources. (*Ebmeier, 2016*).

- Hypothesis: signal = linear combination of statistically independent variables.
- (*Comon, 1994 ; Hyvärinen and Oja, 1997 ; Stone, 2004 ; Ebmeier, 2016*)
  - Maximisation of the statistical independence of sources (ICA)
  - Extraction of low amplitude signals

- InSAR = combination of deformation and noise sources
  - Application of the method sICA (*Gaddes et al., 2018*)
  - fastICA algorithm (*Hyvärinen and Oja 1997 ; Hyvärinen and Oja, 2000*)

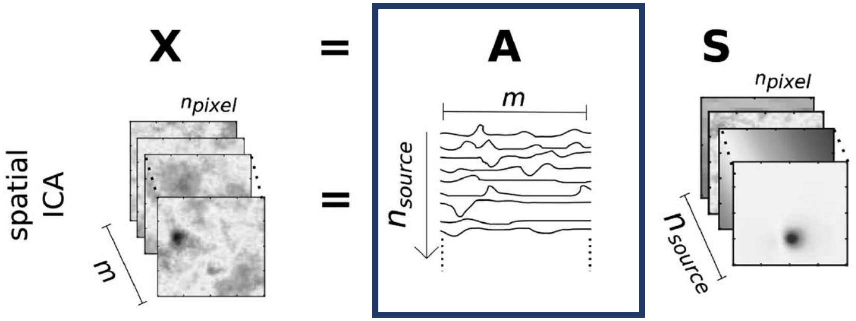

- spatial Independant Component Analysis (sICA)
  - Analysis of **mixing vectors**
  - Switching Edge Detection (*Smith, 1998*; *Roggero, 2012*)
  - Raw time series

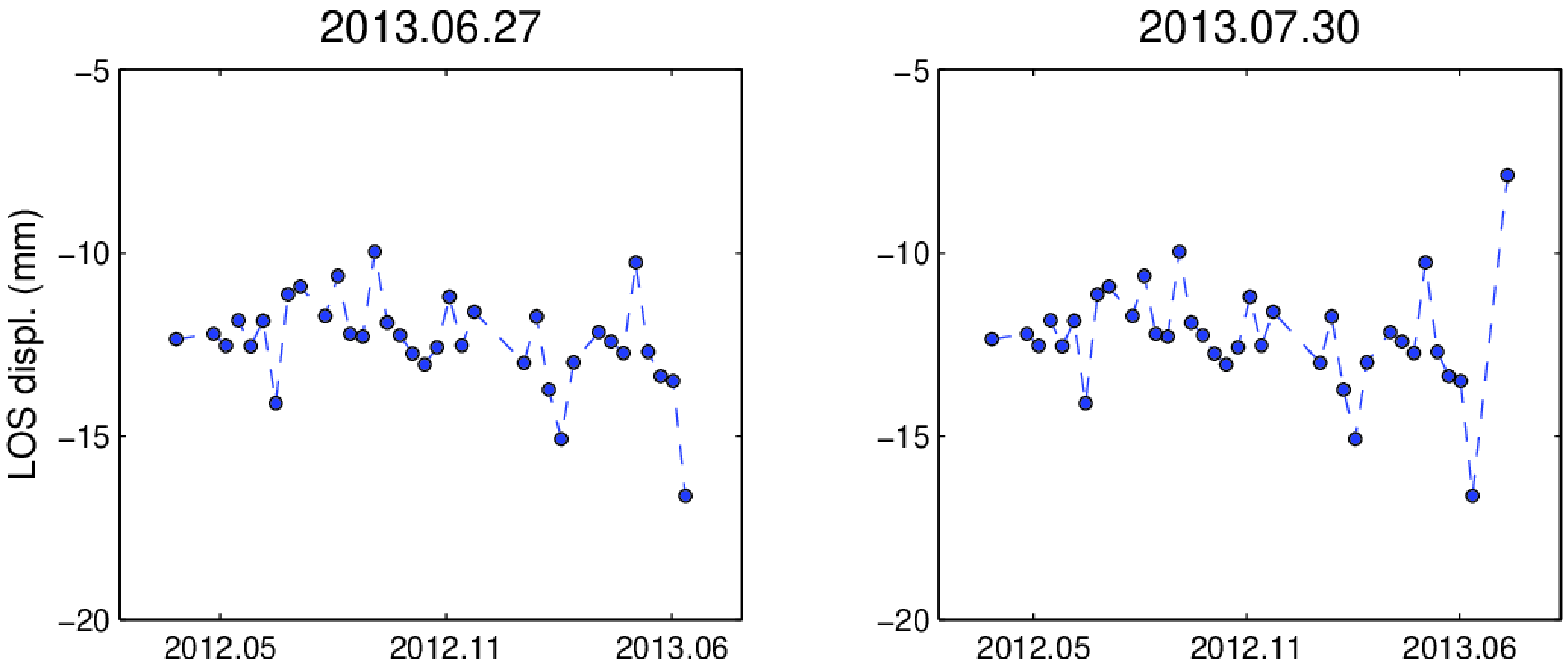

Fig 13. Switching Edge Detection. Step 0: raw time series.

- spatial Independant Component Analysis (sICA)
  - Analysis of **mixing vectors**
  - Switching Edge Detection (*Smith, 1998*; *Roggero, 2012*)

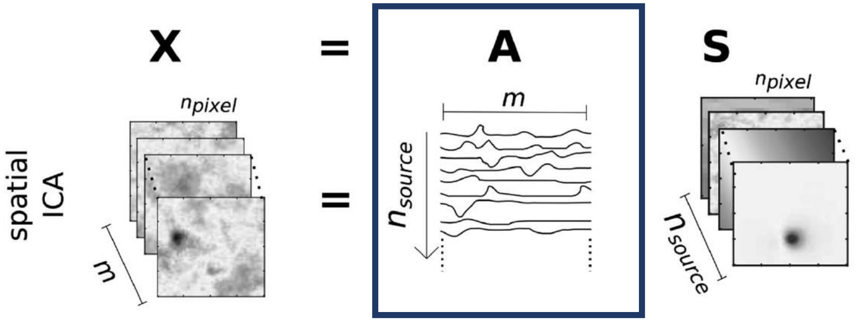

  - Moving averages

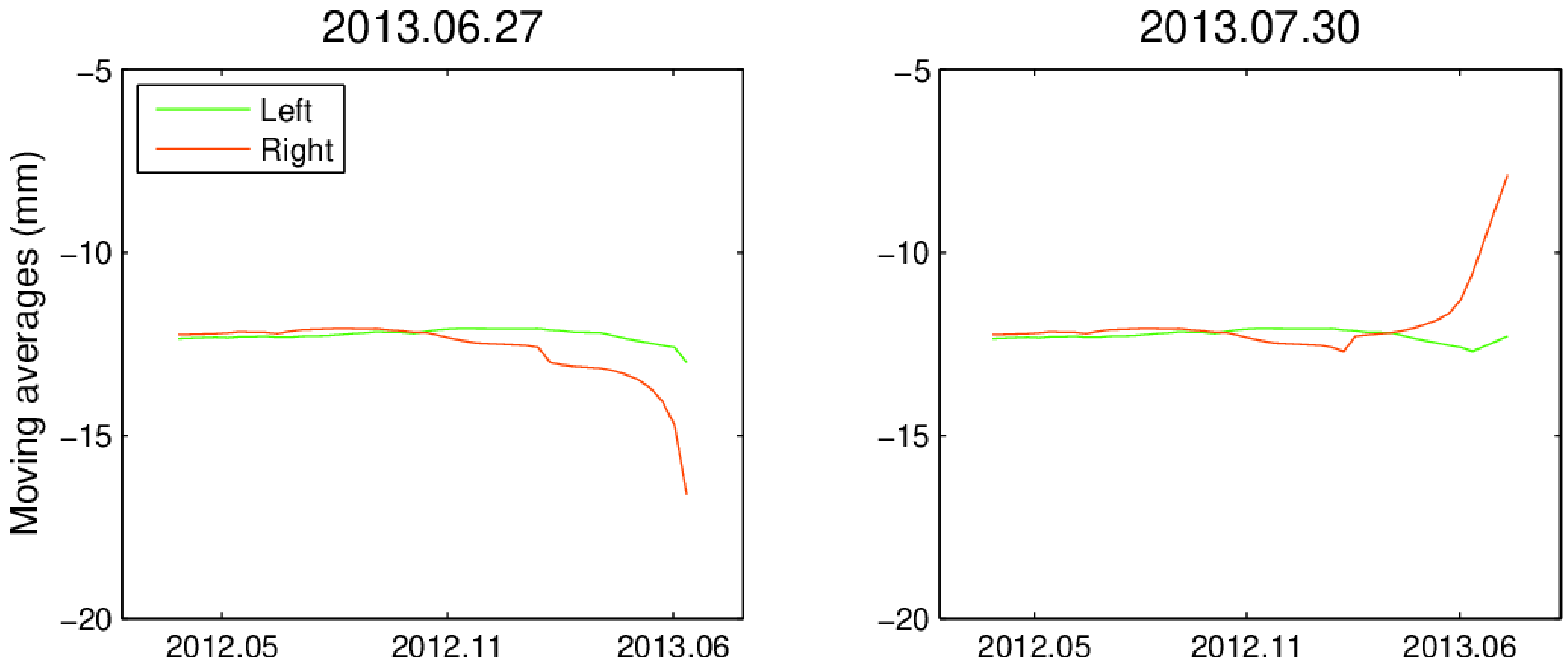

Fig 14. Switching Edge Detection. Step 1: moving averages.

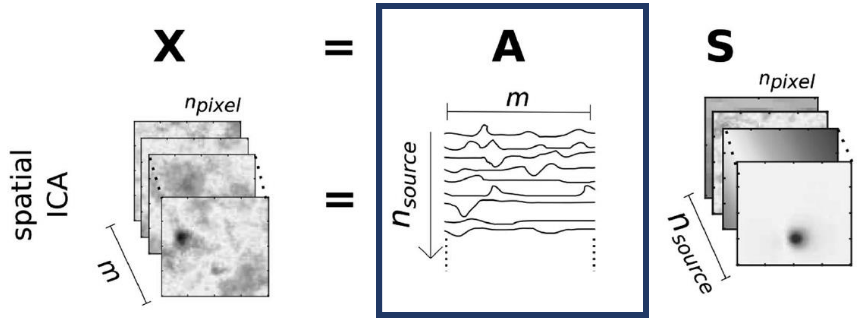

- spatial Independant Component Analysis (sICA)
  - Analysis of **mixing vectors**
  - Switching Edge Detection (*Smith, 1998*; *Roggero, 2012*)
  - Moving variances

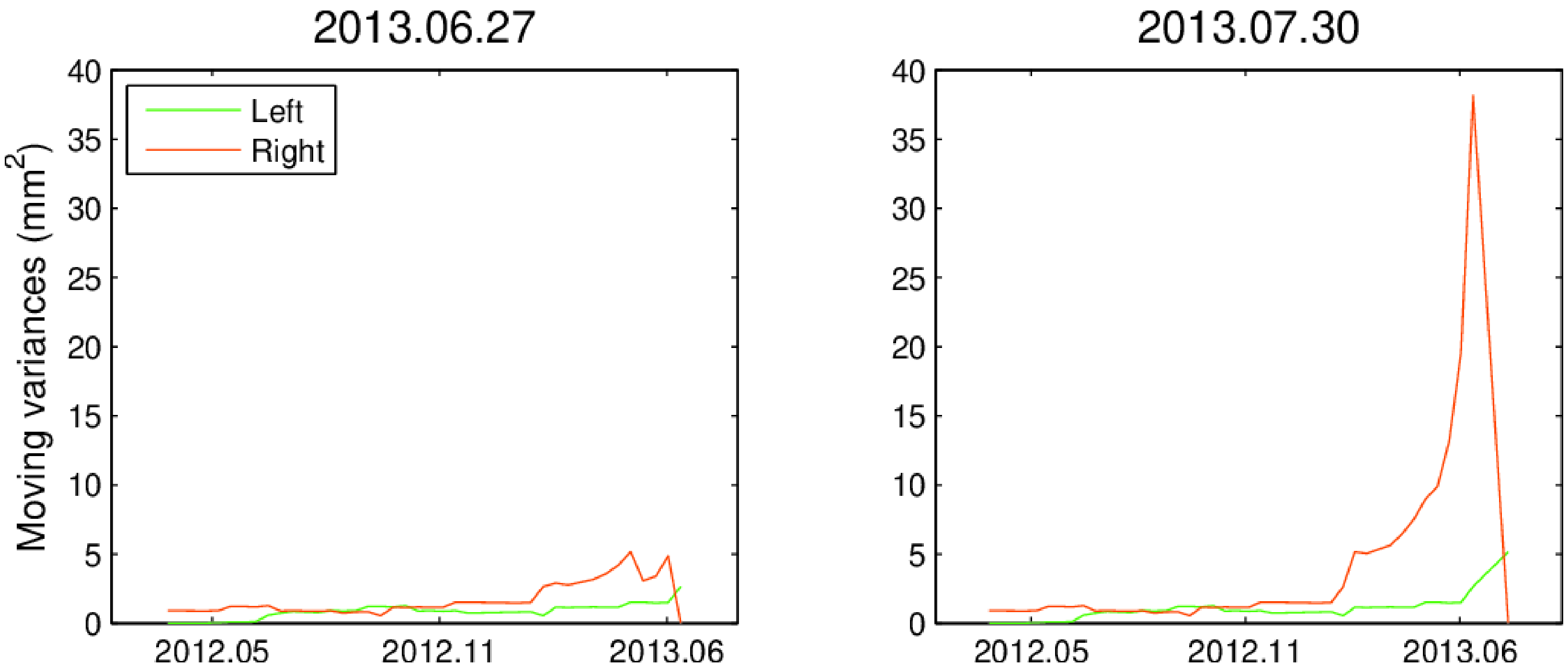

Fig 15. Switching Edge Detection. Step 2: moving variances.

- spatial Independant Component Analysis (sICA)
  - Analysis of **mixing vectors**
  - Switching Edge Detection (*Smith, 1998*; *Roggero, 2012*)

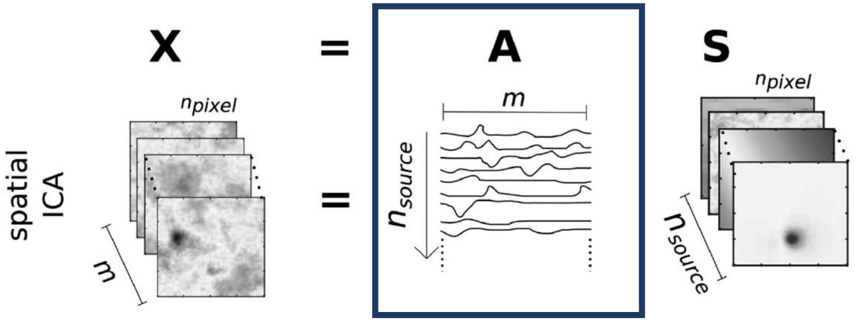

  - Corrected time series

$$H_{out}(t_i) = g_{i+}H_{i+} + g_{i-}H_{i-}$$

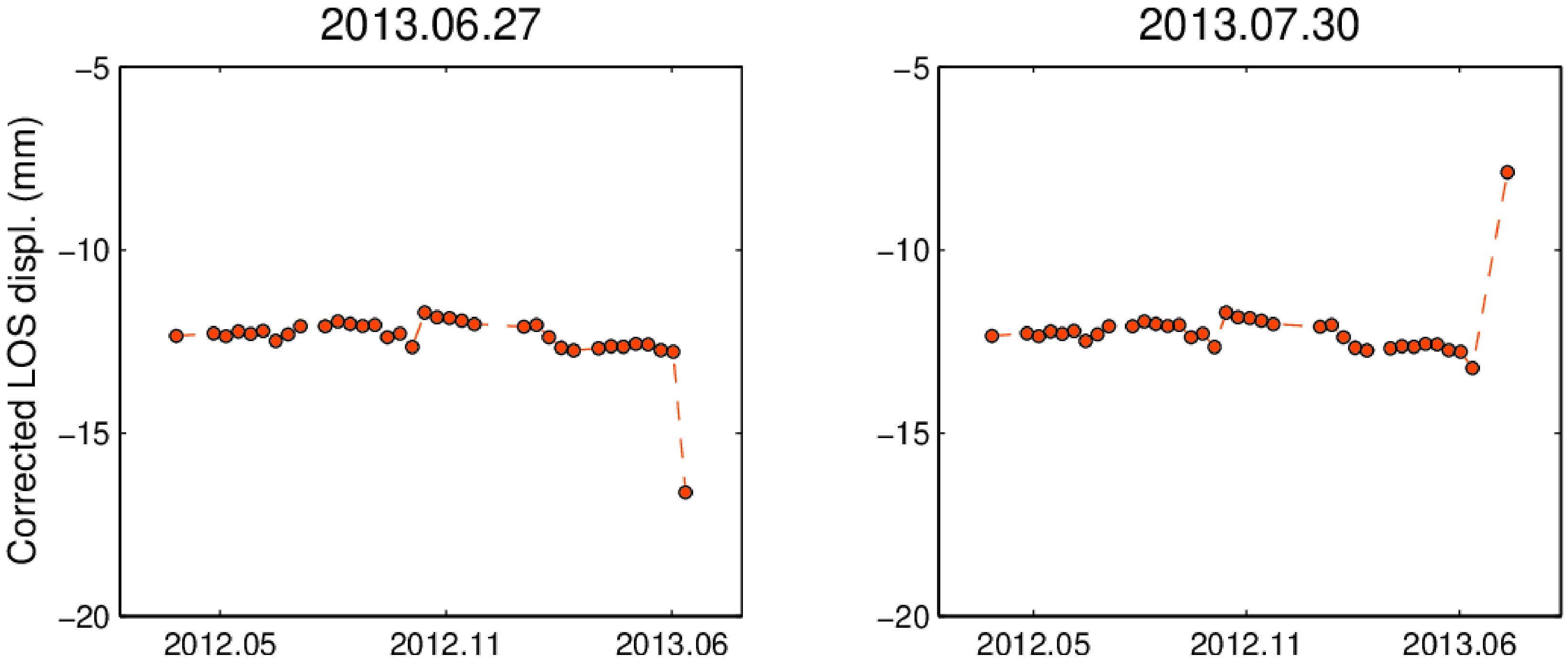

Fig 16. Switching Edge Detection. Step 3: corrected time series.

- spatial Independant Component Analysis (sICA)
  - Analysis of **mixing vectors**
  - Switching Edge Detection (*Smith, 1998*; *Roggero, 2012*)

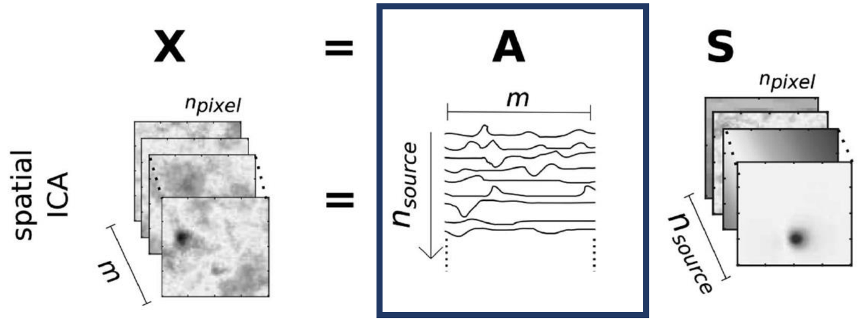

  - Detection function

$$Y(t_i) = \frac{\mid H_{i+} - H_{i-} \mid}{\sigma_{loc}}$$

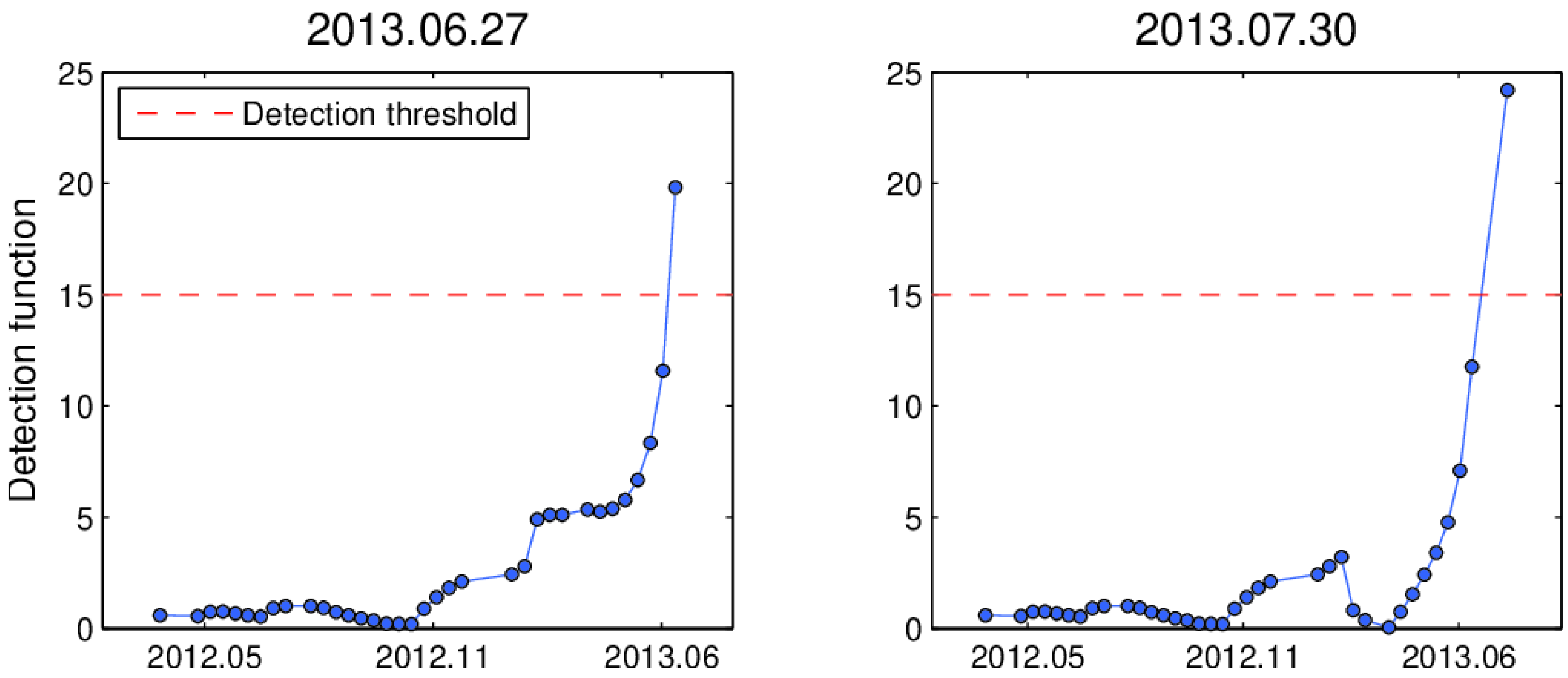

Fig 17. Switching Edge Detection. Step 4: detection function.

5. MONITORING

- spatial Independant Component Analysis (sICA)

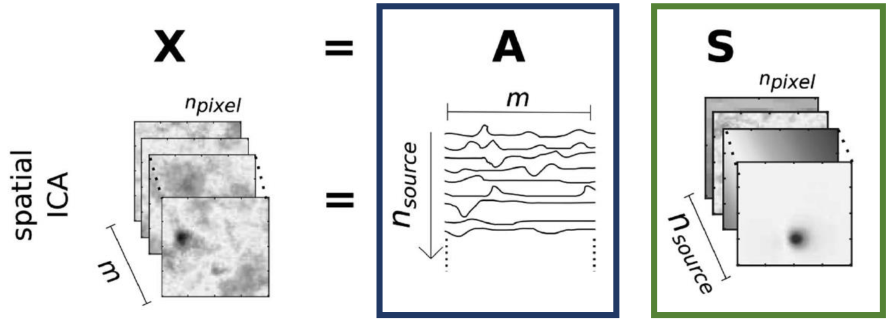

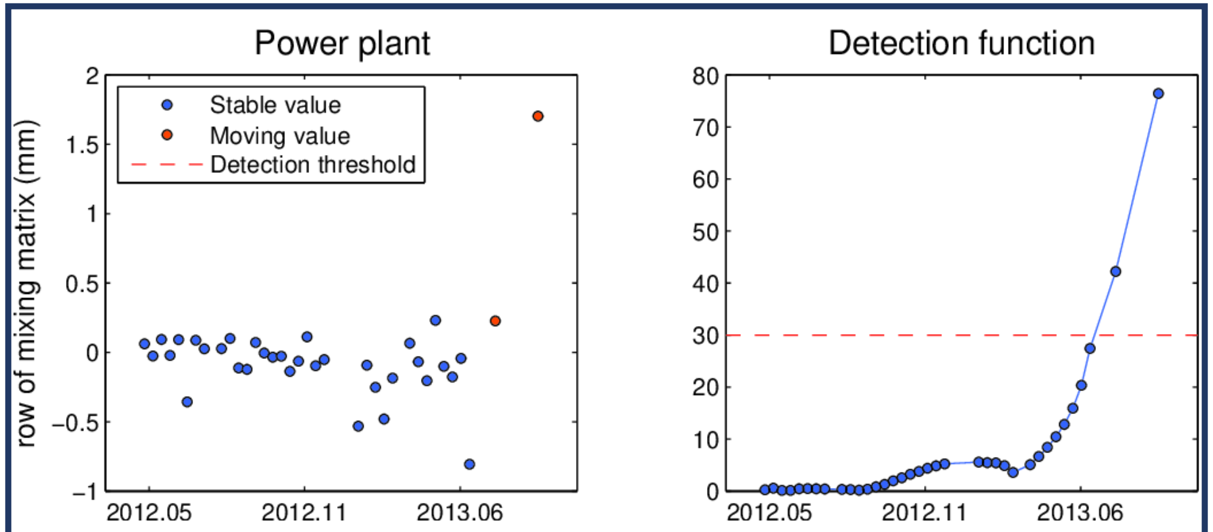

Fig 18. Left: mixing vector with added variance. Right: detection function.

Accident: 2013.06

Detection: 2013.07

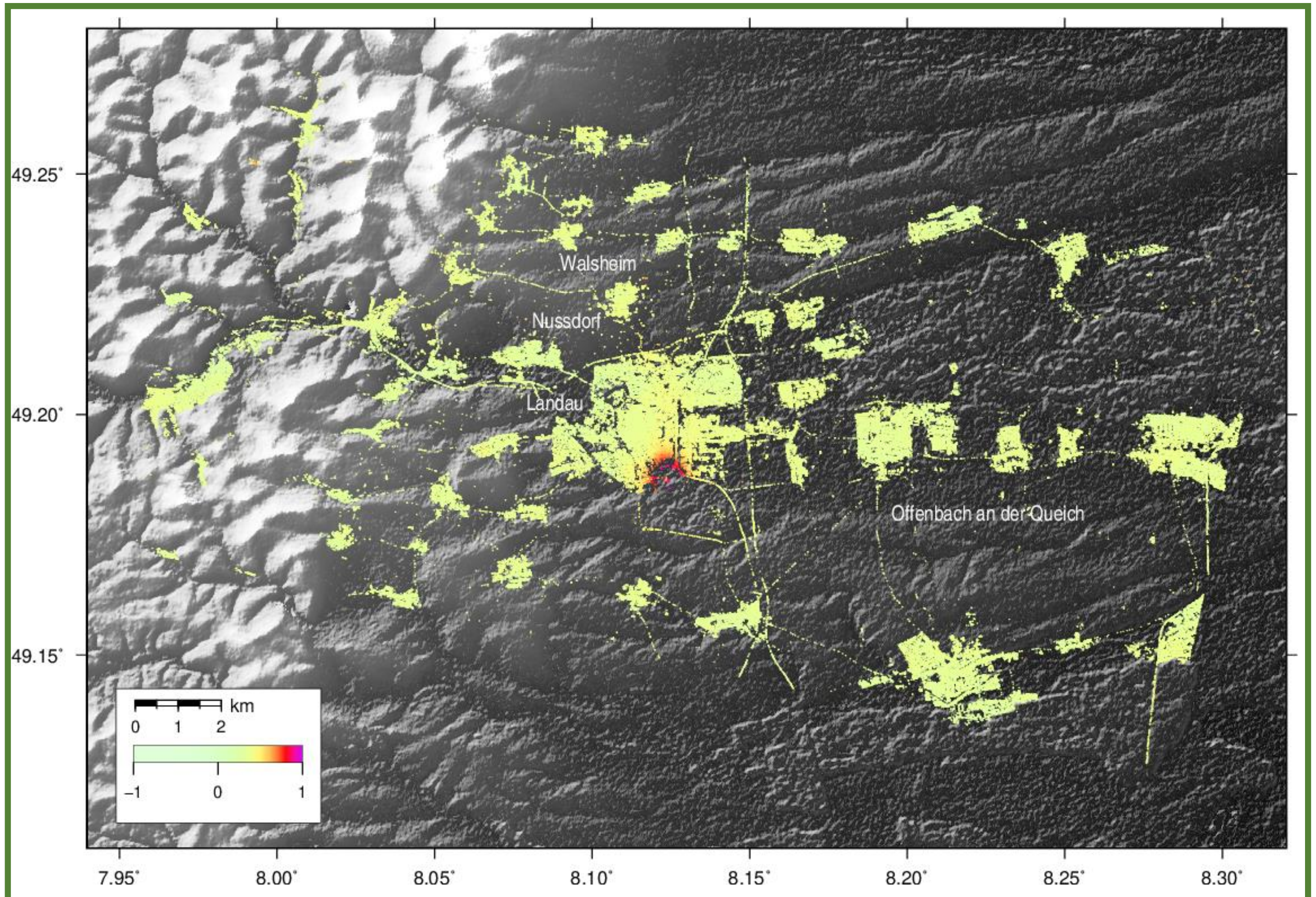

Fig 19. Spatial representation of the source related to the accident.

5. MONITORING

- spatial Independant Component Analysis (sICA)

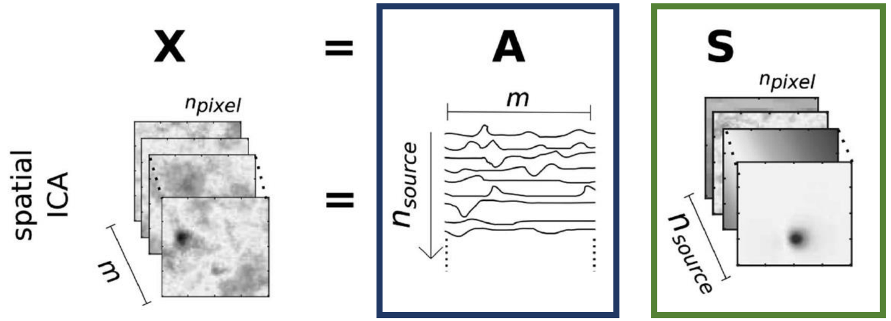

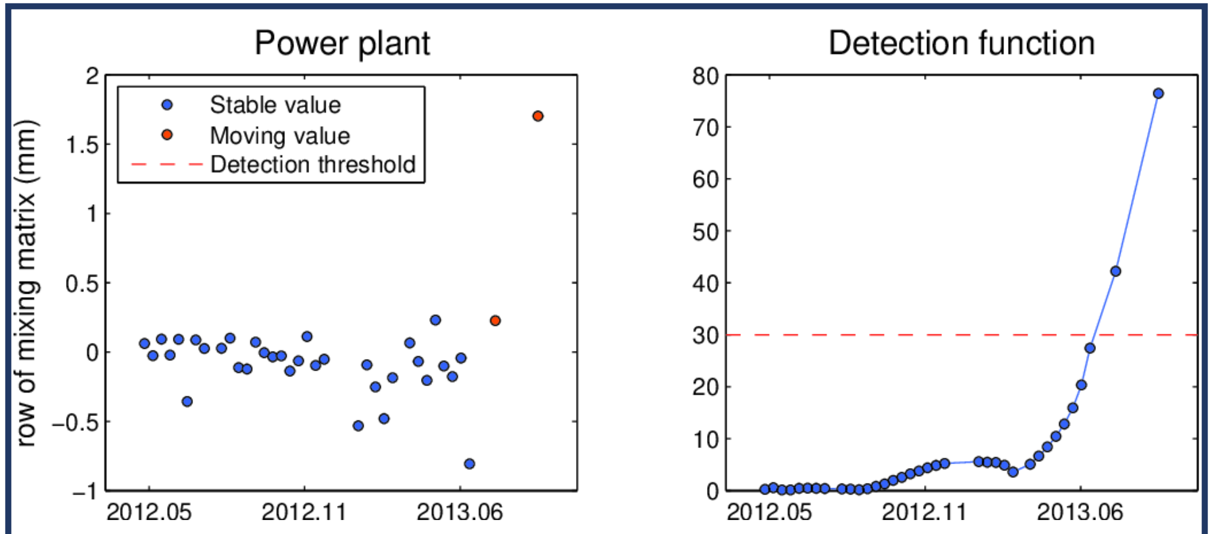

Fig 18. Left: mixing vector with added variance. Right: detection function.

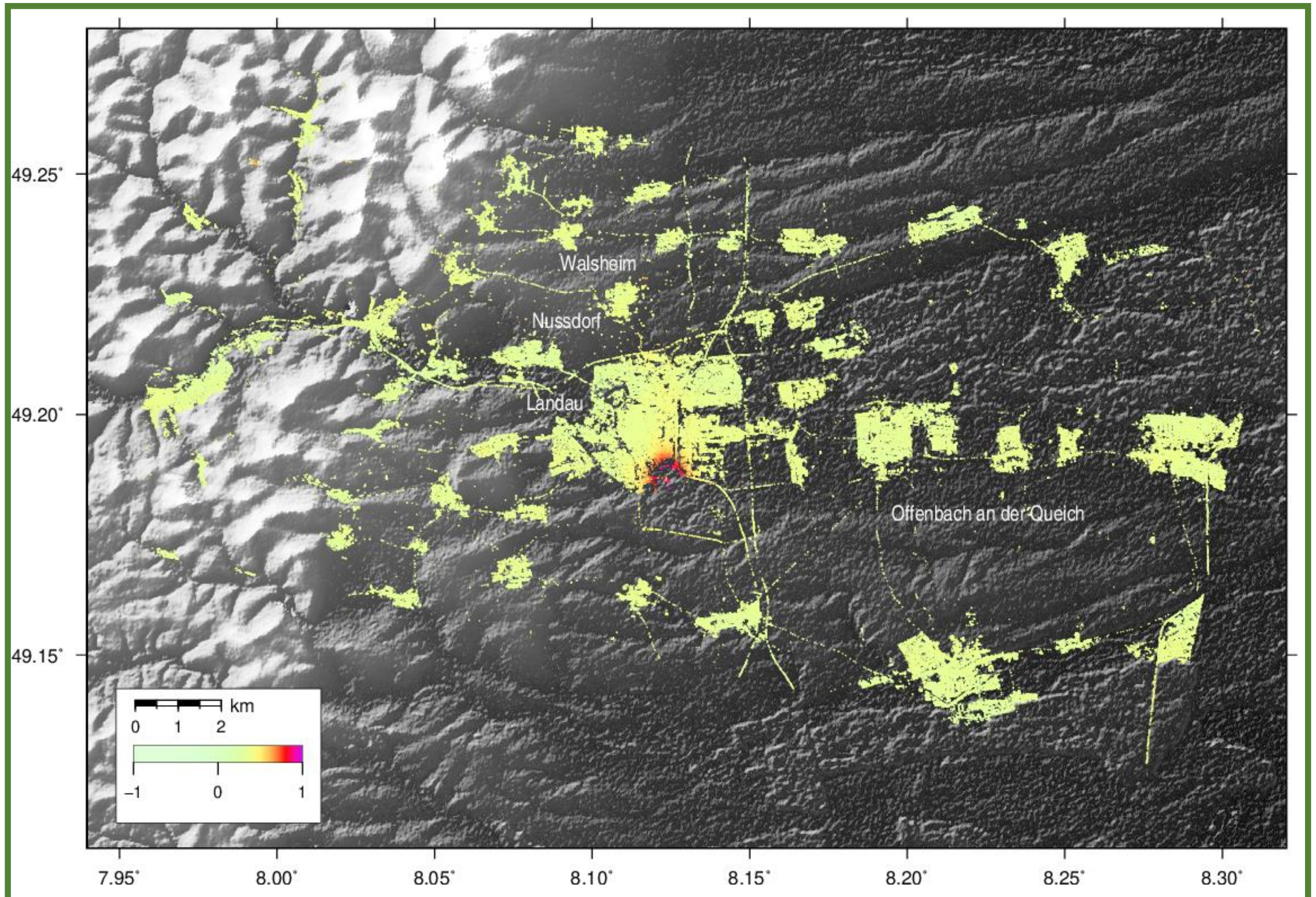

Fig 19. Spatial representation of the source related to the accident.

- **But…**
  - Time-consuming processing
  - Obligation to determine a new *master*
  - … or strong temporal decorrelation
  - ... or limited by geometric constraint (λ / 2)

- **Daisy-chain approach**

- Dataset
  - TerraSAR-X
  - 40 X-band images (λ = 3.1 cm)
  - Repeat period : 11 days

- Method
  - Minimisation of temp. and perp. baselines
  - Coherence mask
  - Spatial referencing
  - Reconstruction of pixel’s time course

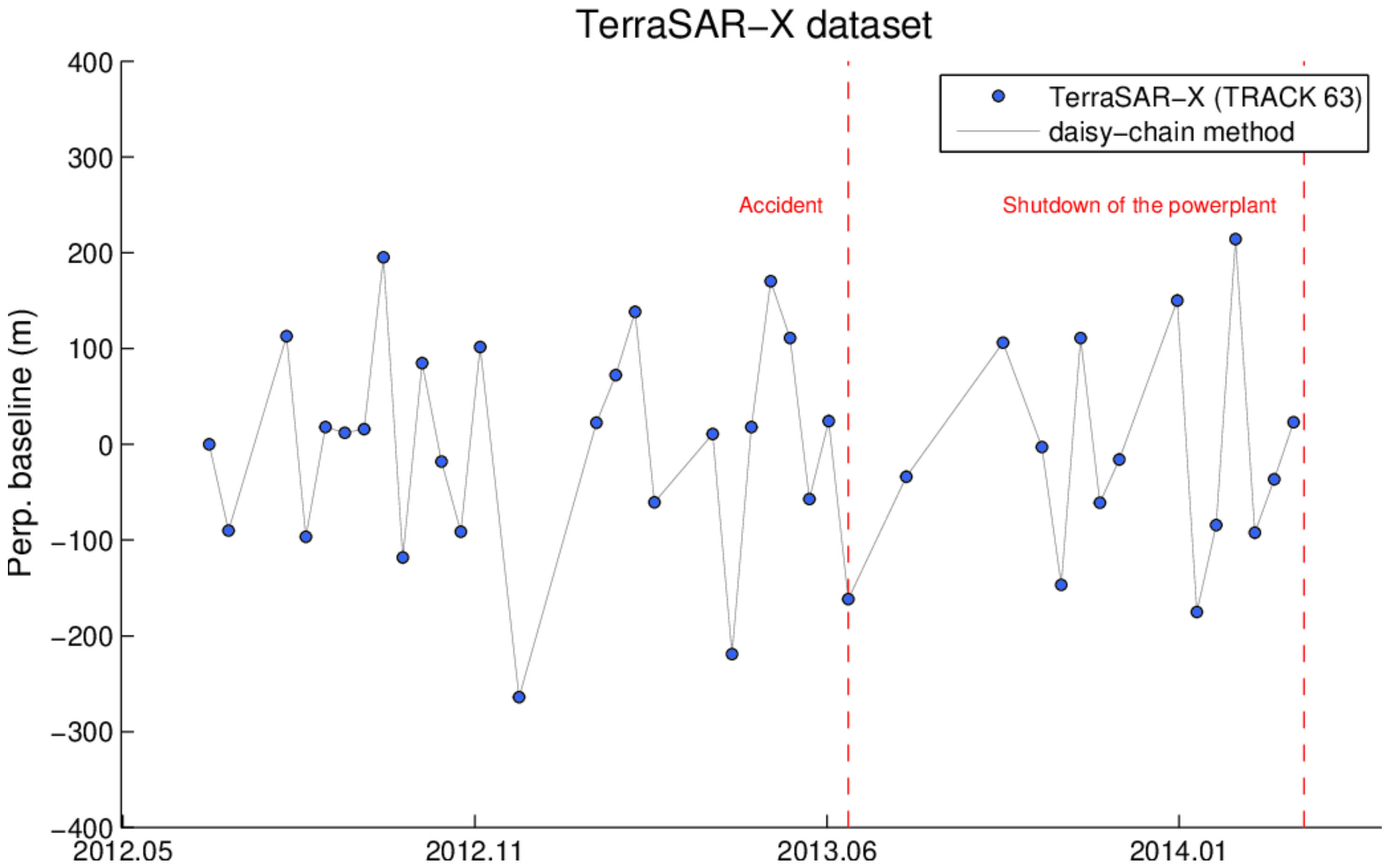

Fig 20. TerraSAR-X dataset: perpendicular baselines as a function of time. Red lines: accident, and of the power plant. Daisy-chain approach

5. MONITORING

- Spatial analysis

- Uplift
  - Geothermal site (~30 mm LOS)
  - Spread over the city (~10 mm LOS)

- Subsidence
  - North-east (~40 mm LOS)

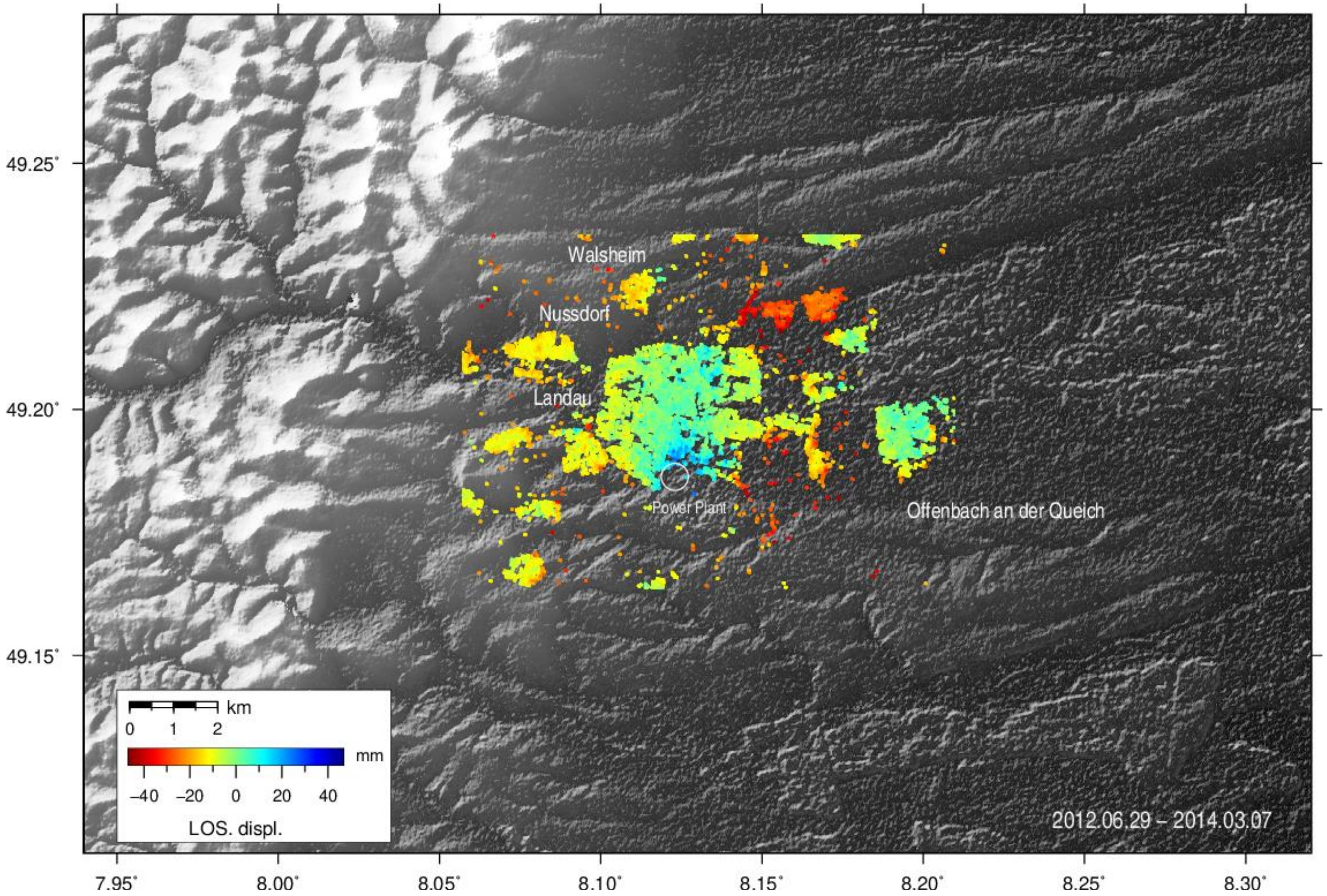

Fig 21. Cumulated LOS displacements, period: 2012.06.29 – 2014.03.07.

- Monitoring

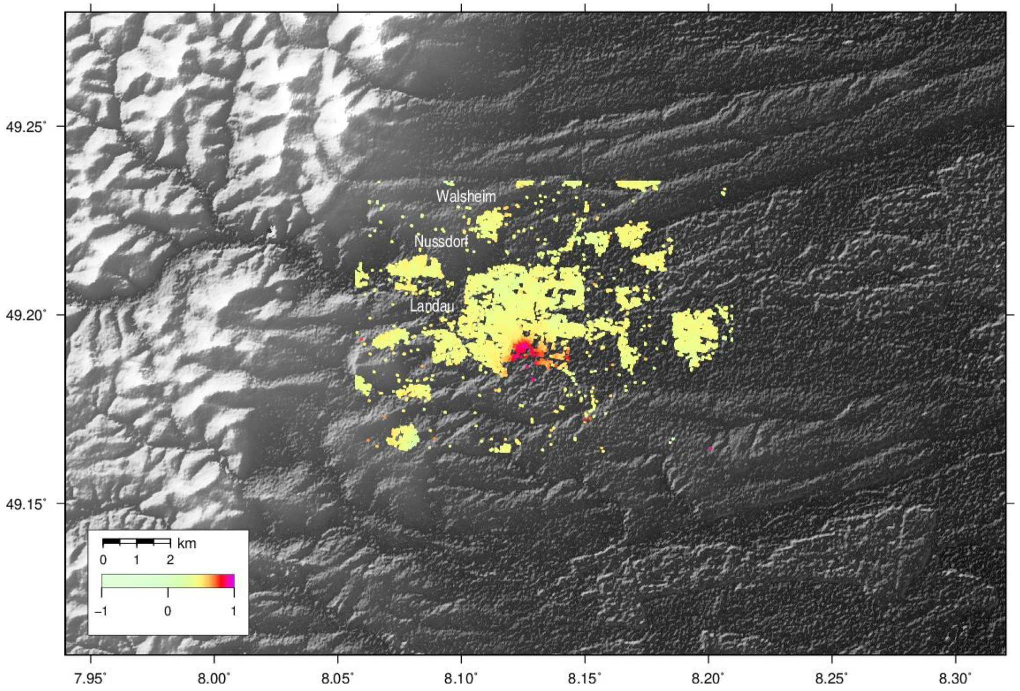

Fig 22. Spatial representation of the source related to the accident.

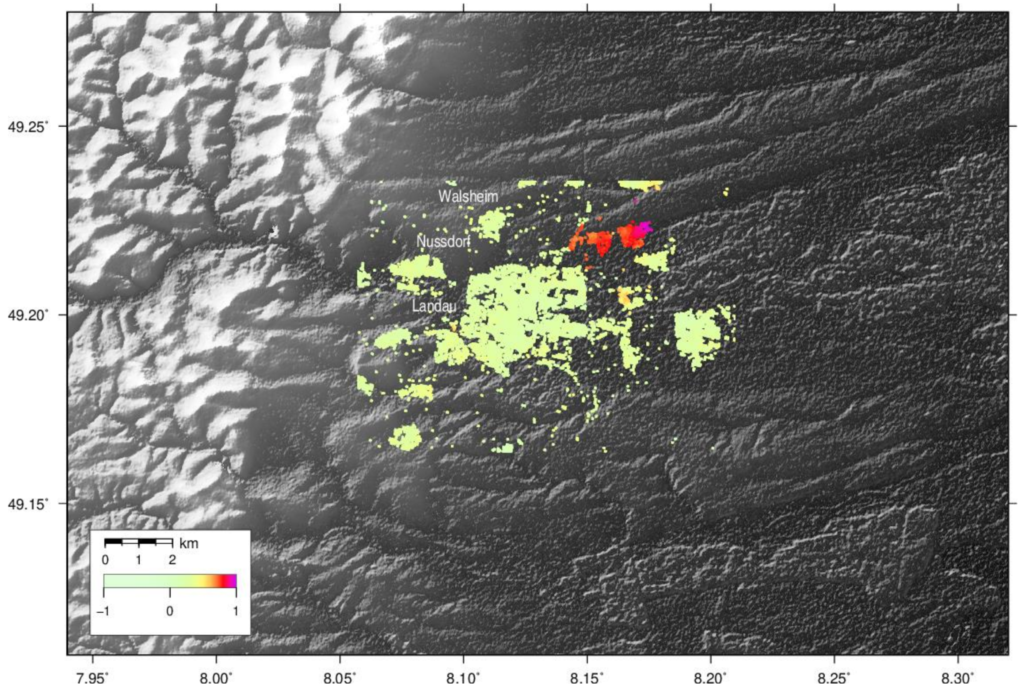

Fig 24. Spatial representation of the source related to the unwrapping error.

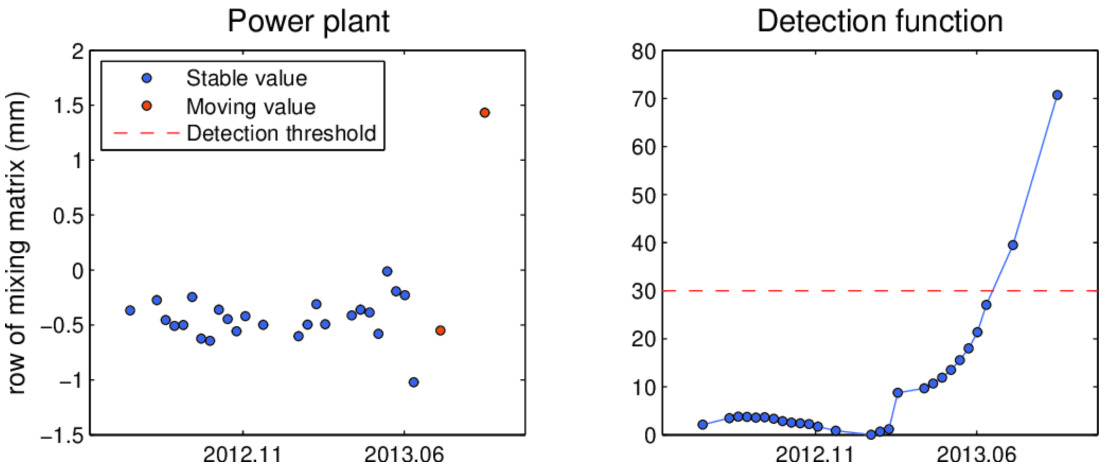

Fig 23. Left: mixing vector with added variance. Right: detection function.

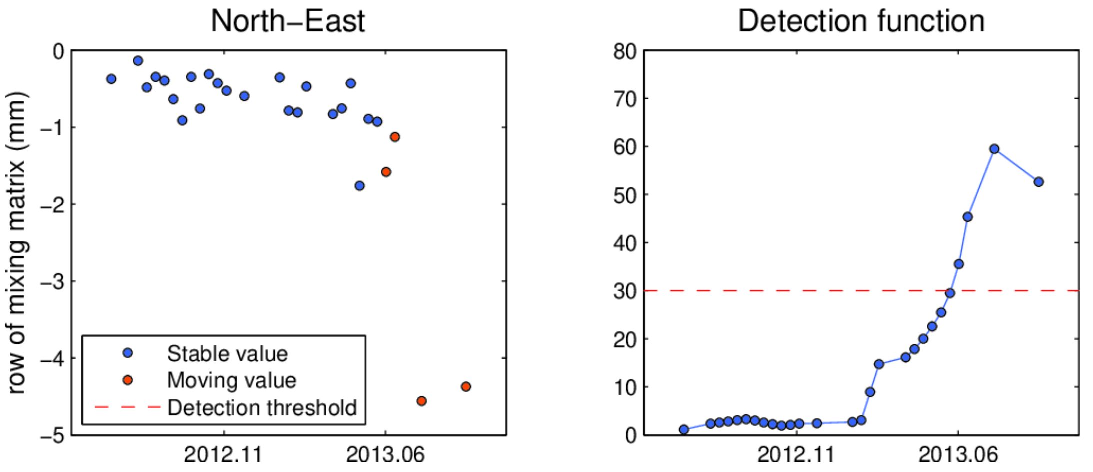

Fig 25. Left: mixing vector with added variance. Right: detection function.

6. CONCLUSIONS AND PERSPECTIVES

- PS-InSAR monitoring approach
  - Advantages
    - Reduction of problem dimension with sICA
    - Efficient detection of abnormal behaviour without “false positive”
  - Disadvantages
    - Time-consuming processing

- Daisy-chain monitoring approach
  - Advantages
    - Minimisation of temp. and perp. baselines
    - Fast processing after the new image acquisition
    - Sufficient accuracy for near real-time monitoring
  - Disadvantages
    - Extremely sensitive to unwrapping errors (especially in vegetated areas)
    - Strong temporal dependence to reconstruct pixel’s time course

6. CONCLUSIONS AND PERSPECTIVES

- Perspectives
  - Application to Sentinel-1 data flow

6. CONCLUSIONS AND PERSPECTIVES

- Perspectives
  - Application to Sentinel-1 data flow
  - Daisy-chain approach with NSBAS (*Doin et al.,2011*)

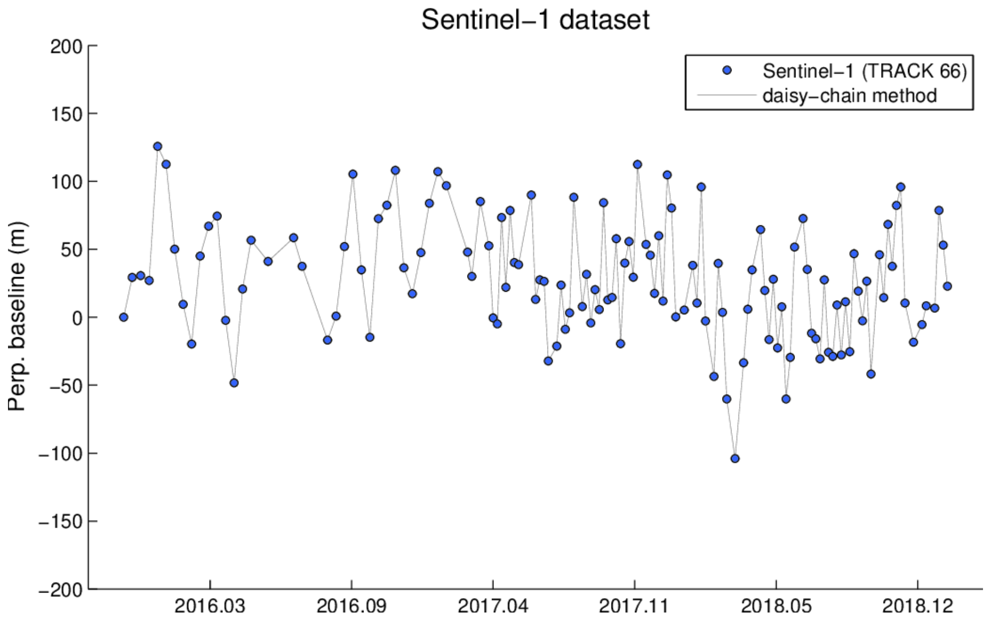

Fig 26. Sentinel-1 dataset: perpendicular baselines as a function of time. Red lines: accident, and of the power plant. Daisy-chain approach

- Perspectives
  - Application to Sentinel-1 data flow
  - Daisy-chain approach with NSBAS (*Doin et al.,2011*)
  - Detection of low-amplitude displacements (post-accident subsidence) enhanced by machine-learning (*Gaddes et al., 2019*)

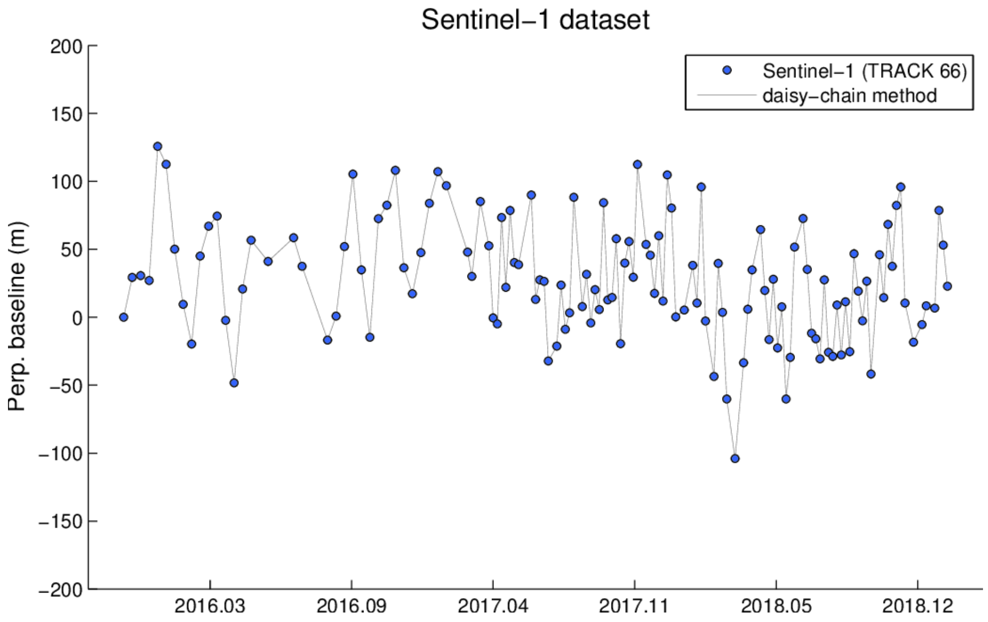

Fig 26. Sentinel-1 dataset: perpendicular baselines as a function of time. Red lines: accident, and of the power plant. Daisy-chain approach

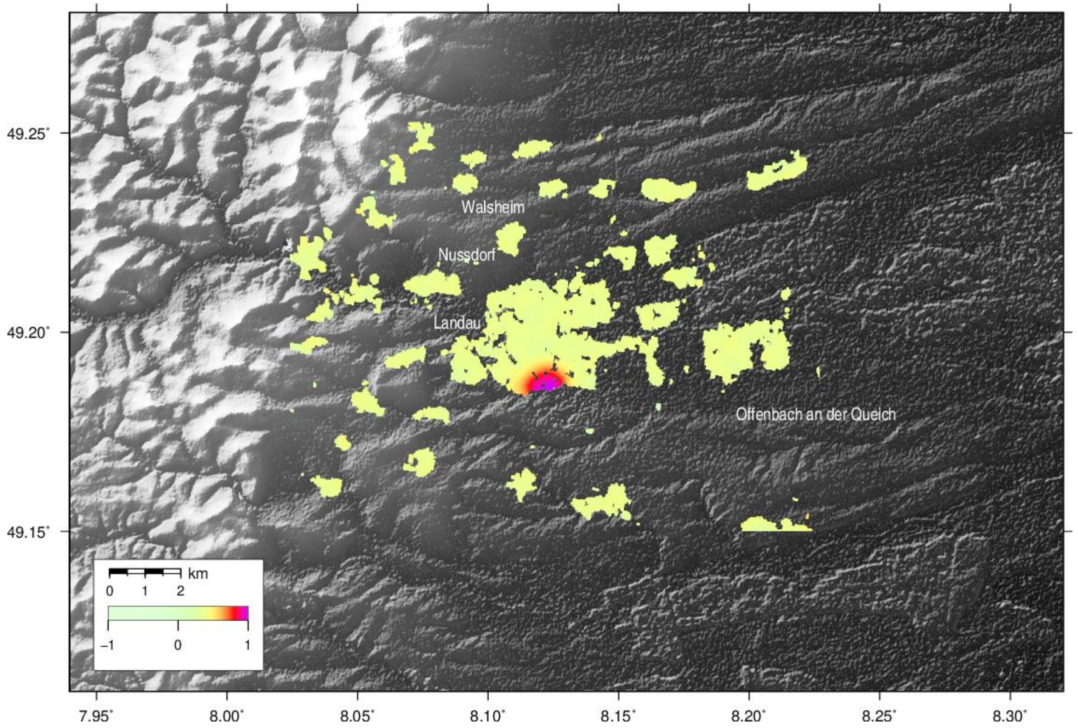

Fig 27. Spatial representation of the source related to the accident.

6. CONCLUSIONS AND PERSPECTIVES

- Perspectives
  - Application to Sentinel-1 data flow
  - Daisy-chain approach with NSBAS (*Doin et al.,2011*)
  - Detection of low-amplitude displacements (post-accident subsidence) enhanced by machine-learning (*Gaddes et al., 2019*)
  - Spatial resolution improved by new pixel selection techniques (*Spaans and Hooper, 2016*)

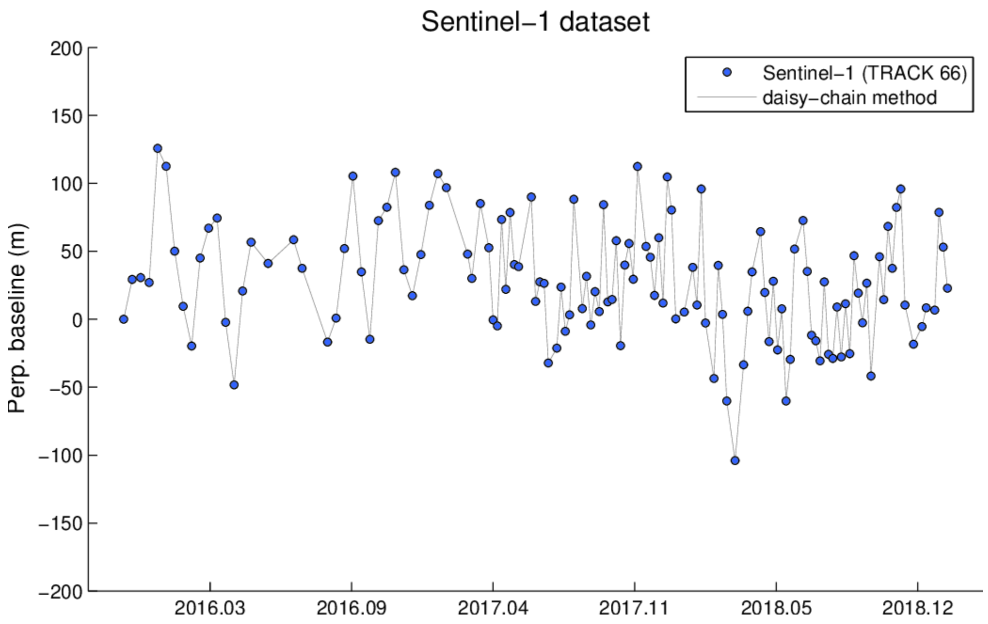

Fig 26. Sentinel-1 dataset: perpendicular baselines as a function of time. Red lines: accident, and of the power plant. Daisy-chain approach

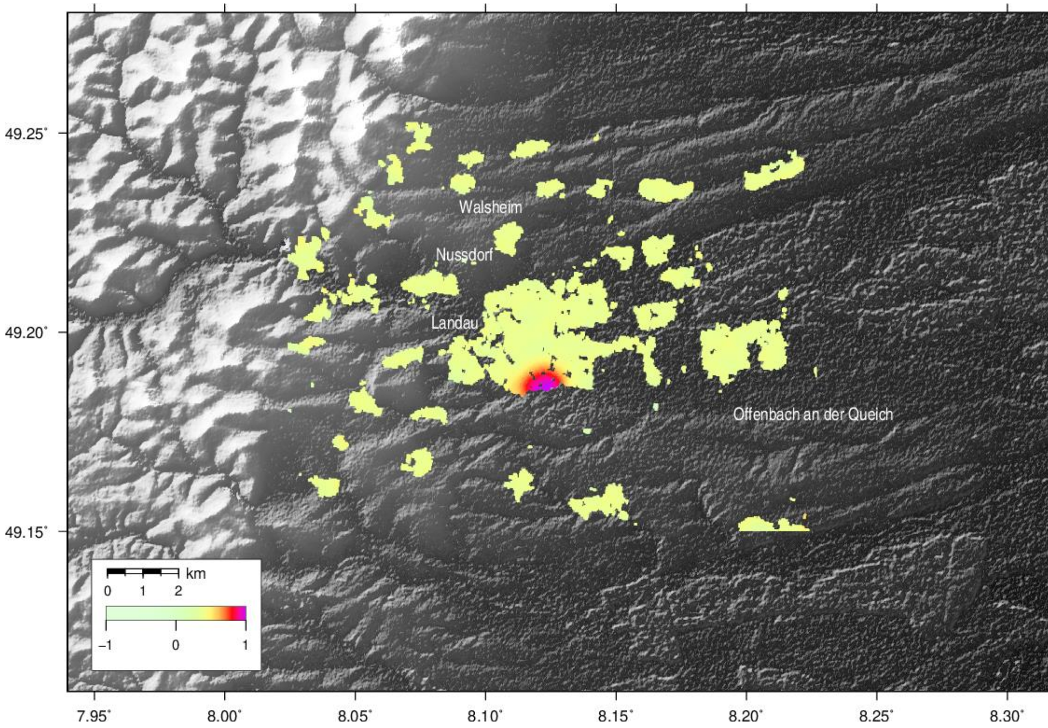

Fig 27. Spatial representation of the source related to the accident.